Appendix G—Paleoseismic Sites Recurrence Database

By Ray J. Weldon, II,[1] Timothy E. Dawson,[2] Glenn Biasi,[3] Christopher Madden,[4] and Ashley R. Streig[1]

Introduction

As part of the Uniform California Earthquake Rupture Forecast, version 3 (UCERF3), an effort was made to identify new sites with earthquake recurrence data and update or revise the UCERF2 database where new data made this appropriate. The results of this compilation are summarized in table G1, and the complete dataset can be found in tables G2 (all new and revised data) and table G3 (superseded data). These tables contain the same information that was included in the Microsoft Excel spreadsheet entitled: "UCERF3Paleosites_V2" that was distributed early in the UCERF3 process for subsequent analysis, including the development of recurrence intervals and associated formal uncertainties, as described in other appendixes (especially appendix H, this report). To keep clear exactly what has changed since UCERF2 (largely presented in appendix B, this report), we separated the data into tables G2 and G3 here and there are tabs in the Excel input file labeled "OLD" for the original UCERF2 data that is no longer being used, and "NEW" that contain the updated data used in the current analysis.

This appendix also includes two derivative tables (tables G4 and G5) and a methodology for estimating the probability of overlap between sites from rupture offset, either measured or estimated from the recurrence intervals. Table G4 shows how many of the dated age ranges of paleoearthquakes from sites along the same fault overlap. Table G5 allows a comparison of recurrence intervals determined by dating paleoearthquakes with recurrence intervals calculated by dividing average offset per event (data from appendix R, this report) by slip rate, and estimates of the likelihood of events correlating between sites on the same fault. Likely rupture extent is based on average offset. Initially, it was hoped that these data would be directly used in the inversion, but due to limitations in time, they were not formally incorporated; however, they did serve as useful checks on the inversion results and led to small changes in the inversion parameters to better match the recurrence and displacement per event data.

Paleoseismic Sites Recurrence Database

This appendix is, in part, an update to the paleoseismic recurrence database used in UCERF2 (Dawson and others, 2008b). We have retained the format used by Dawson and others (2008), keeping the entries that have not been superseded and adding new entries for new and revised sites. Within tables G2 and G3, each site has its own subtable or worksheet and includes

[1]University of Oregon.
[2]California Geological Survey.
[3]University of Nevada, Reno.
[4]Oregon State University.

information regarding site locations, event ages, uncertainties, and the average interval of time between earthquakes, calculated simply as the time period spanned by the record divided by the number of complete intervals (excluding open intervals). Event ages are reported as calendar ages or years before present, where "Old" is the start of the age range and "Young" is the end of the event age range. "Open" refers to the open interval since the most recent event.

An uncertainty range of the interval between events is also reported, with the minimum interval ("Min interval") as the time between the oldest constraining age of the youngest event and the youngest constraining age of the oldest event. Where the event ages overlap, this is reported as zero years. The maximum interval ("Max interval") is reported as the time between the youngest age of the younger event and the oldest age of the older event. "Mid" (or "preferred") is typically the middle of the reported interval range, unless the mean age was calculated from a probability density function (PDF) that has a most likely value, and is commonly referred to in the literature as the preferred time interval. It should be noted that, because the earthquakes that define the intervals could have occurred at anytime during their reported age range, the mid-point of the interval range may not be a meaningful number. While Bayesian analysis programs such as OxCal are able to generate actual PDFs of event ages and intervals, we did not always have direct access to the radiocarbon dates that are necessary to construct quantitative models that would provide the PDFs. Thus, the values given as "Mid" should not be considered a statistically determined mean for the range of the interval. However, in the absence of a full PDF, the mid can be used if one decides to assign a Gaussian-shaped PDF to the range. For example, at the Indio paleoseismic site, Biasi and others (2009) only had the reported age ranges of Sieh (1986) to use, so they assigned Gaussian-shaped PDFs for each event age. We therefore include the mid values for convenience if someone wishes to generate similar PDFs.

For most sites we report a recurrence interval calculated by the average interval method (total time of closed paleoseismic intervals divided by the number of observed intervals) used in UCERF2. "Time max" and "Time min" are reported in years and are taken from the dates that constrain the paleoseismic record. "AI max" and "AI min" represent the range of recurrence calculated from the constraining ages. "AI preferred" is the middle of the range reported for recurrence (with the same caveats for "Mid"). Because the paleoseismic data were compiled for UCERF3 in order to generate recurrence estimates using more statistically based methods (see appendix H, this report), we did not systematically update this data for all of the newer and revised entries. However, we include these estimates in the table where they already existed or we added them as a point of comparison to recurrence estimates generated by other methods.

There are relatively few faults where there are enough data to compare different methods of calculating recurrence intervals or where one can compare the event rate along strike to see how rapidly intervals vary. The best place to make this comparison is along the southern San Andreas fault, shown in figure G1. The average recurrence interval increases fairly systematically to the south with steps associated with the major fault junctions with the San Jacinto and eastern California fault zones, where one might expect the recurrence interval to change because the slip rate does. Recurrence intervals calculated from the data and assuming a log-normal recurrence distribution model (fig. G1, green points with error bars) tend to be longer because the average interval approach does not include the long open interval and may undersample rare long intervals in our short event series. Recurrence intervals calculated from average offsets and the geologic slip rate (fig. G1, red squares) agree well with those determined from the average dated intervals. This agreement suggests that the geologic slip rate,

displacement per event, and recurrence intervals based on the ages of paleoearthquakes are internally consistent. This agreement is important because it suggests that difficulties satisfying both the slip rates and recurrence intervals encountered in the Grand Inversion are likely due to other factors in the inversion.

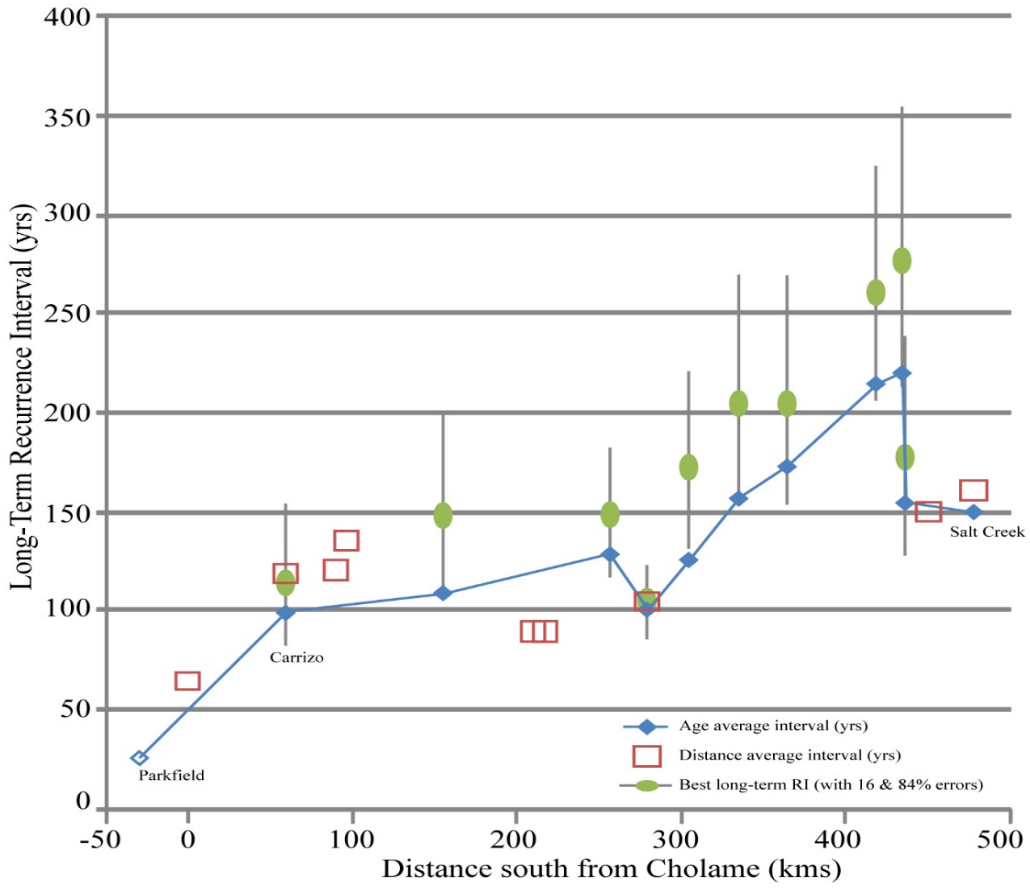

Figure G1. Comparison of three methods for calculating recurrence intervals. Green ovals are from appendix H (this report), calculated with a log-normal distribution model, with 16 percent and 84 percent confidence ranges. Blue diamonds, connected by the blue line, are recurrence intervals for paleoseismic sites calculated as the average time interval between observed events. Red squares are recurrence intervals calculated by dividing the average slip per event (from appendix R, this report) by the geologic slip rate of the fault at that point. Given the limitations of the methods and very short event series, agreement is quite good. Interestingly, the average recurrence interval varies quite smoothly along the fault, suggesting that the data are robust. The steeper steps in this trend are at the junction with the San Jacinto fault, at kilometer ~280, and the eastern California shear zone, at kilometer ~430, where the slip rate on the San Andreas fault changes.

Correlations Between Paleoseismic Sites

Traditionally, and in previous working groups, correlation of paleoearthquakes between sites along a fault was inferred by overlap of the ages of paleoearthquakes and the geometry of the fault between sites. If the geometry was simple and the ages overlapped, continuity in rupture was usually assumed, and if the geometry was complex or ages did not overlap, a segment

boundary was inferred. In UCERF2, faults with adequate recurrence information (called "A-faults") were thus segmented (Weldon and others, 2008; Dawson and others, 2008a; Wills and others, 2008). While segmentation is not explicitly assumed in UCERF3, correlation between sites can provide a powerful test of the validity of the model; if the model predicts many (or few) overlaps in rupture between sites, we should see many (or few) overlaps in age in the paleoearthquakes at the sites. For this reason we compiled age overlap data in table G4. We determined the common time interval for all pairs of sites along faults with multiple sites, recorded the number of events at each site in the common interval, and then recorded the number of events with overlapping age. While age overlap only permits correlation, lack of overlap in age precludes correlation, and differences in the number of events in a common time interval provide a minimum estimate of nonoverlapping events. The overlap numbers in table G4 provided a qualitative estimate of overall correlation between sites that were compared with the model results as part of the overall assessment of the grand inversion model.

The fact that seismic ruptures have a significant spatial extent means that at least semi-quantitative methods can be proposed to estimate probabilities of correlation based on independent observations of paleoseismic rupture displacements. For this reason we compiled in table G5 the distances between sites along faults with multiple paleoseismic and average displacement per event sites, and used the average displacement per rupture, either measured (from appendix R, this report) or calculated from the average recurrence interval and slip rate at the site, to estimate the probability that rupture will extend between the site pairs.

We consider two cases under which a probability of correlation of ground rupture can be estimated. In the first case, displacements d_1 and d_2 are assumed to be available at two paleoseismic sites, S_1 and S_2. In the second case we consider what might be done if the data consist only of average displacements d_{a1} and d_{a2} are available at their respective sites. In both cases the uncertainties are large, such that the results are perhaps best interpreted as informed expectations.

Case 1: Observed Displacements at S_1 and S_2

For this case we assume that the dates of displacements d_1 and d_2 are uncertain, but in such a way as to allow correlation but not to prove it. We also assume that the dates of any other paleoseismic events in either site chronology are sufficiently separated that if the events correlate, only one match is allowed.

The probability of correlation based on observed displacement involves three components. First, $P(L|d)$ (fig. G2; Biasi and Weldon, 2006; Biasi and others, 2011) is the probability of rupture length L associated with observed displacement d. A subscript indicating the paleoseismic site may be added where the association of d or L is required for clarity. A general correlation of L with average rupture displacement is well established (for example, Wells and Coppersmith, 1994). The relationship of an observed displacement to the rupture average is more complex because it depends on where the observation site is within the rupture, on rupture displacement variability within ruptures, and on the assumed distribution of ground rupture sizes. For example, a 2-meter displacement is more likely to be near the center of a M6.8 rupture, and near the ends of a larger event, say a M7.6. At the same time, natural variability of rupture displacements within a given rupture means that a 2-meter displacement might occur in the middle of the M7.6, even though 3.5 meters might be more typical. Biasi and Weldon (2006) describe the process of inverting observed rupture variability relating d to rupture average displacement d_a, and use Wells and Coppersmith (1994) to relate d_a to L. The inversion depends

on the magnitude-frequency distribution considered to span the space of possible sources of ground rupture. Figure G2 assumes that earthquakes of any magnitude are equally likely at the observation point. Comparable relations assuming characteristic and Gutenberg-Richter (GR) magnitude-frequency distributions produce, respectively, somewhat longer and shorter correlation lengths (Biasi and Weldon, 2006).

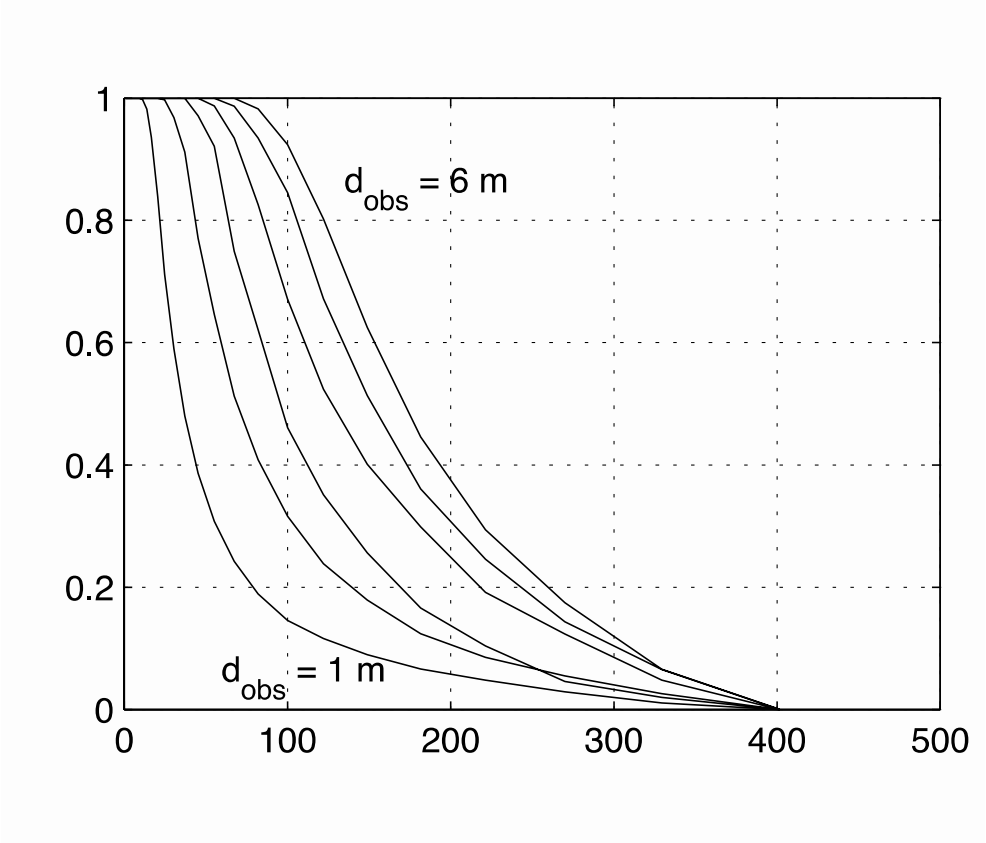

Figure G2. Probability of rupture length given an observed displacement. Modified from Biasi and Weldon (2006) for the case that ruptures of any size are equally likely. $P(L|d_{obs})$ assumes ignorance about where d_{obs} is in the rupture, so 2 meters, say, could be a peak in an *M*6.8 rupture, or a tail of an *M*8. Probabilities cross at small probabilities because of the fine scale structure of probability of displacement given magnitude, p(d|*M*). See Biasi and Weldon (2006) for details.

The second component, $P(S_2|L_1(d_1))$, refers to the probability that site 2 is within a rupture of length L_1. If the rupture known at S_1 is assumed to extend at random in either direction along the fault, the probability that it reaches to S_2 can be suggested from geometric considerations. This probability should increase with L_1 and increase as the separation between S_1 and S_2 decreases. Technically it has to reach with enough displacement there to be detected, but considering the rate of decay of slip at the ends of most ruptures, neglecting this detail should not substantially affect the probabilities. For the limited information case assumed here, L_1 is assumed to be a function of d_1. Figure G3 gives the probability of a rupture reaching to an adjacent site 2 as a function of rupture length if site 1 occurs at random within the rupture.

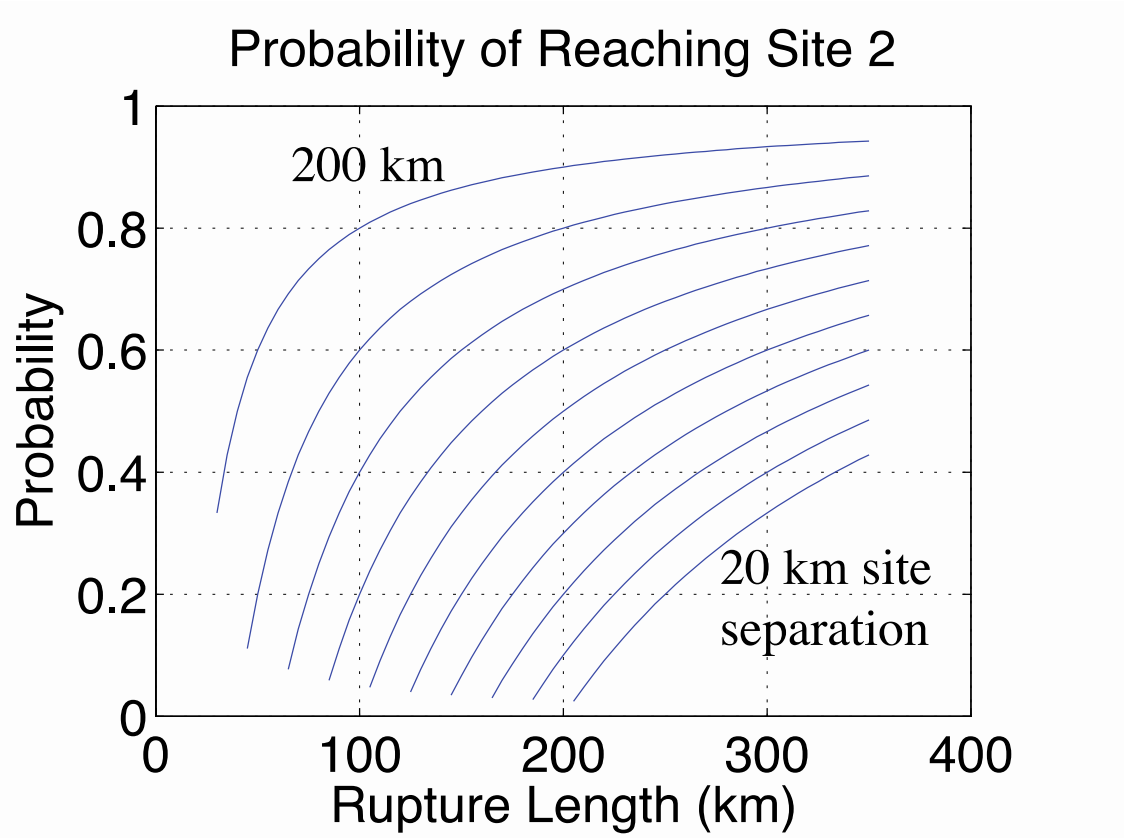

Figure G3. Probability that a rupture observed at site 1 and associated with some rupture length will reach to a second site. Site 1 is assumed to be located at random inside the rupture. Contour lines correspond to various separations between site 1 and site 2, in 20 kilometer (km) increments. Figure modified from Biasi and others (2011).

The third component, $P(d_2 \text{ at } S_2)$, is the probability that displacement is detected at site 2. For the present case observation of d_2 is assumed and $P(d_2 \text{ at } S_2)$ is assumed to be 1.

The three components contributing to the probability of event correlation given observations of displacements d_1 and d_2 is then:

$$P_c = P(\text{correlation; } S_1, S_2|d_1,d_2) = P(L_1|d_1) * P(S_2|\, L_1(d_1)) * P(d_2 \text{ at } S_2) \quad (1)$$

Figure G4 summarizes equation 1 for various observed displacements d_1. Plainly each component in equation 1 has substantial uncertainty. On the other hand, the functional forms of the curves in figure G4 are fairly intuitive. Ruptures with large displacements extend farther and are more likely to involve multiple sites. Small observed displacements have less predictive power about what may be present down the fault.

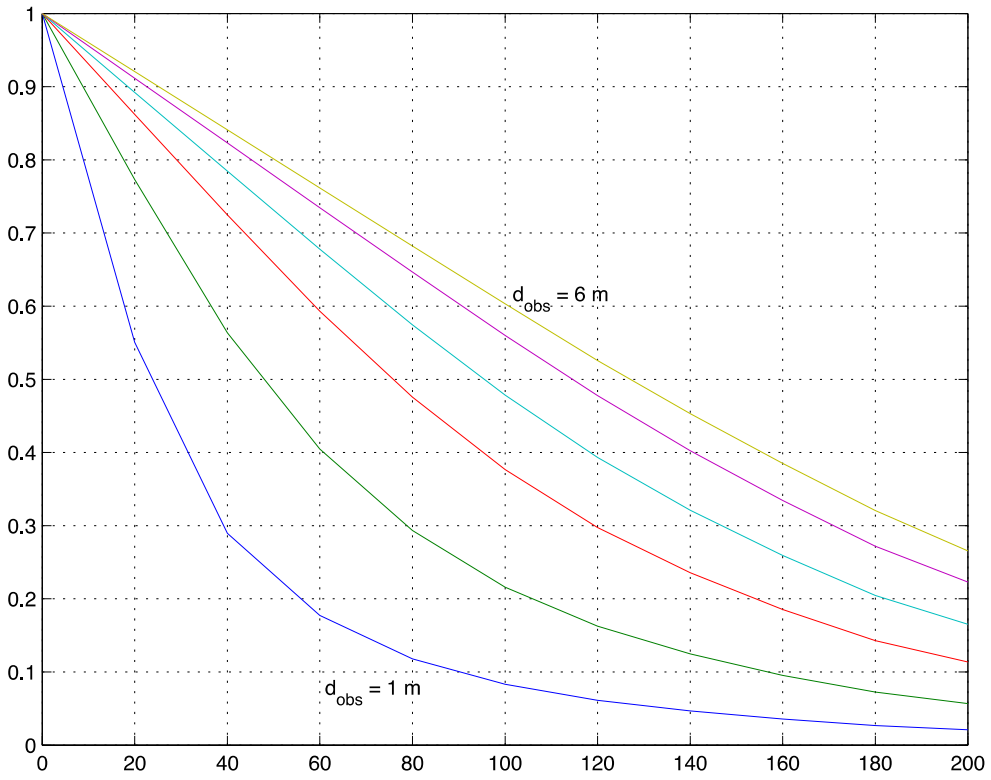

Figure G4. Combination of relationships shown in figures G2 and G3 into a single plot from which the probability of correlation can be estimated from site separations and observed displacements.

The joint probability of correlation given observations of both d_1 and d_2 and date correspondence is higher than if the correlation is taken either displacement separately. With the probability of noncorrelation $P_{c1}' = (1-P_{c1})$, the joint probability is (1-probability that both miss). The misses based on P_{c1} and P_{c2} are uncorrelated, so we have the probability of correlation as:

$$P_{c12} = (1-P_{c1}' * P_{c2}') \quad (2)$$

Thus, if the probability at S_1 given d_1 is 70 percent and the probability at S_2 given d_2 is 60 percent, we have the probability of correlation $P_{c12} = (1-0.3*0.4) = 88$ percent. Equation 2 applies when the event date probability distribution functions overlap and have the resolution to say that if they correlate, only this correlation is allowed.

Case 2: Average Displacements at S1 and S2

Case 2 differs from case 1 in two respects. First, $P(L|d)$ will differ when average displacement d_a is used in place of d. Second, event dating is not available, so consideration of correlation depends on displacements alone. Qualitatively, the lack of dating evidence for correlation decreases probabilities of correlation and confidence in them.

Probability $P(L|d)$ (fig. G2) was developed assuming that d was drawn at random from within the rupture that caused it. How exactly to adjust $P(L|d)$ for use with average site

displacements (that is, $P(L|d_a)$), is less clear. Associating average displacement d_a with d in $P(L|d)$ could underestimate rupture length because $P(L|d)$ includes the case where the observation comes from a peak displacement of a small rupture. It might also be that $P(L|d) \sim P(L|d_a)$ because, as an average, lengths will be distributed around the mean. Finally, if we examine variability in normalized ruptures, more of the rupture length is above the average than below it (appendix F, this report). In this case $P(L|d_a)$ may slightly overestimate L. The adjustment of $P(L|d)$ will also depend on the assumed magnitude distribution (Biasi and Weldon, 2006). Resolving this adjustment in detail is a research question beyond the scope of UCERF3. For now, $P(L|d_a)$ is assumed to be similar to $P(L|d)$ in figure G2.

Probabilities of correlation between sites with average displacements interact with the event rates or recurrence intervals (RIs) of the sites being compared. The site with the lower recurrence interval is more influential because it sets an upper limit on the rate of events occurring at both sites. Specifically, the correlation shouldn't predict over 100 percent. With this in mind, we estimate the correlation rate from a weighted average of the separate predicted correlation rates, with a check that the predicted fraction doesn't exceed 100-percent of the lower RI site.

$$P_{c12}(d_{a1}, d_{a2}) = (1-P_{c1}' * P_{c2}') * \max(RI_1, RI_2)/\min(RI_1, RI_2) \quad (3)$$

Results are given in the right side of the matrices in table G5. As discussed above for table G4, these results were used as a reality check on the results of the inversion. Model overlap frequencies were compared with expected overlap for individual faults and large discrepancies were identified and investigated. We believe that the kinds of constraints developed in tables G4 and G5 could (and should) be used directly in future inversions but time constraints on UCERF3 did not permit the approach to be developed adequately to be formally included.

Acknowledgments

We greatly appreciate reviews by David Schwartz, Gordon Seitz, and Tom Rockwell and discussion with many members of the UCERF3 team, especially Ned Field and Morgan Page. We thank Kevin Milner for some technical assistance, and Keith Knudsen and Tran Huynh for help editing and keeping us on schedule. This project was supported in part by SCEC grants 157576 and 119939.

References

Akçiz, S., Grant-Ludwig, L., and Arrowsmith, J.R., 2009, Revised dates of large earthquakes along the Carrizo section of the San Andreas Fault, California—since A.D. 1310±30: Journal of Geophysical Research, v. 114, no. B01313.

Akçiz, S.O., Grant, L.B., Arrowsmith, R.J., Zielke, O., Toke, N.A., Noriega, G., Cornoyer, J., Starke, E., Rousseau, N., and Campbell, B., 2006a, Does the new paleoseismological evidence from the Carrizo Plain section of the San Andreas Fault indicate abnormally high late Holocene slip rates? [abs.]: Eos (American Geophysical Union Transactions), v. 87, Fall meeting supplement, abs. T21E-01.

Akçiz, S., Grant, L.G., and Arrowsmith, J.R., 2006b, New and extended paleoseismological evidence for large earthquakes on the San Andreas fault at the Bidart Fan site, California [abs.]: Seismological Research Letters, v. 77, no. 2, p. 268.

Akçiz, S., Grant, L.B., Arrowsmith, J.R., Zielke, O., Toke, N.A., Noriega, G., Stark, E., and Cornoyer, J., 2005, Constraints on ruptures along the San Andreas fault in the Carrizo plain—initial results from 2005 Bidart Fan site excavations: Earthquake Center Annual Meeting, Proceedings and Abstracts, v. 15, *http://www.scec.org/meetings/2005am/*.

Allen, C.R., and others, 1972, Map showing surface ruptures created at the time of and after the Borrego mountain earthquake of April 9, 1968: U.S. Geological Survey Professional Paper 787, plate 1.

Arrowsmith, J.R., Madden, C., Haddad, D.E., Salisbury, J.B., and Weldon, R.J., 2011, Compilation of slip in last earthquake data for high-slip rate faults in California for input into slip dependent rupture forecast [abs.]: Eos (American Geophysical Union Transactions), v. 92, Fall meeting supplement, abs. S13B-06.

Arrowsmith, J.R., McNally, K., and Davis, J., 1997, Potential for earthquake rupture and M7 earthquakes along the Parkfield, Cholame, and Carrizo segments of the San Andreas fault: Seismological Research Letters, v. 68, no. 6, p. 902–916.

Bakun, W.H., 2006, Estimating locations and magnitudes of earthquakes in southern California from modified Mercalli intensities: Bulletin of the Seismological Society America, v. 96, p. 1278–1295, doi:10.1785/0120050205.

Barrows, A.G., Kahle, J.E., Weber, F.H., Jr., and Saul, R.B., 1973, Map of surface breaks resulting from the San Fernando, California, earthquake of February 9, 1971 *in* Murphy, L.M., scientific coordinator, San Fernando, California, earthquake of February 9, 1971: National Oceanic and Atmospheric Administration, Environmental Research Laboratories, v. 3, p. 127–135.

Beanland, S., and Clark, M.M., 1994, The Owens valley fault zone, eastern California, and surface rupture associated with the 1872 earthquake: U.S. Geological Survey Bulletin 1982, v. 4, p. 29.

Biasi, G.P., Weldon, R.J., II, and Scharer, K.M., 2011, Rupture length and paleomagnitude estimates from point measurements of displacement—a model-based approach, chap. 9 *of* Audemard, F.A., Michetti, A.M., and McCalpin, J.P., eds., Geological criteria for evaluating seismicity revisited—Forty years of paleoseismic investigations and the natural record of past earthquakes: Geological Society of America Special Paper 479.

Biasi, G., and Weldon, R.J., II, 2009, San Andreas fault rupture scenarios from multiple paleoseismic records—"Stringing pearls": Bulletin of the Seismological Society America, v. 99, p. 471–498, doi:10.1785/0120080287.

Biasi, G.P., and Weldon, R.J., II, 2006, Estimating surface rupture length and magnitude of paleo-earthquakes from point measurements of rupture displacement: Bulletin of the Seismological Society America, v. 96, no. 5, p. 1612–1623.

Biasi, G.P., Weldon, R.J. II, Fumal, T.E., and Seitz, G.G., 2002, Paleoseismic event dating and the conditional probability of large earthquakes on the southern San Andreas fault, California: Bulletin of the Seismological Society America, v. 92, p. 2761–2781.

Biasi, G.P., and Weldon, R.J. II, 2000, Paleoseismic date refinement and implications for seismic hazard estimation, *in* Noller, J.S., Sowers, J.M., and Lettis, W.R., eds., Quaternary geochronology—Methods and applications: Washington, D.C., American Geophysical Union Reference Shelf 4, v. 4, p. 517–520, doi:10.1029/RF004.

Brothers, D.S., Kent, G.M., Driscoll, N.W., Smith, S.B., Karlin, R., Dingler, J.A., Harding, A.J., Seitz, G.G., and Babcock, J.M., 2009, New constraints on deformation, slip rate, and timing of

the most recent earthquake on the west Tahoe-Dollar Point fault—Lake Tahoe basin, California: Bulletin of the Seismological Society of America, v. 99, p. 499–519.

Budding, K.E., Schwartz, D.P., and Oppenheimer, D.H., 1991, Slip rate, earthquake recurrence, and seismological potential of the Rodgers Creek fault zone, northern California: Geophysical Research Letters, v. 18, p. 447–450.

Buga, M.T., Rockwell, T.K., and Salisbury, J.B., 2011, Preliminary paleoseismic results from southern Clark fault, San Jacinto fault zone, southern California—Comparison to the Hog Lake paleoseismic record [abs.]: Southern California Earthquake Center Annual Meeting Proceedings and Abstracts, Palm Springs, Calif., v. 21, *http://www.scec.org/meetings/2011am/*.

Carver, G.A., and Burke, R.M., 1988, Trenching investigations of northwestern California faults—Humboldt Bay region: U.S. Geological Survey Final Technical Report, National Earthquake Hazards Reduction Program, 51 p.

Clark, M.M., 1972, Surface rupture along the Coyote Creek fault, the Borrego mountain earthquake of April 9, 1968: U.S. Geological Survey Professional Paper 787, p. 55–86.

Davis, T.L., 1983, Late Cenozoic structure and tectonic history of the western "Big Bend" of the San Andreas fault and adjacent San Emigdio mountains: University of California, Santa Barbara, Ph.D. Dissertation, 123 p.

Dawson, T.E., Rockwell, T.K., Weldon, R.J., II, and Wills, C.J., 2008a, Summary of geologic data and development of A-Priori rupture models for the Elsinore, San Jacinto, and Garlock faults, appendix F, *of* [WGCEP] 2007 Working Group on California Earthquake Probabilities, contributors, Uniform California Earthquake Rupture Forecast, version 2 (UCERF2): U.S. Geological Survey Open-File Report 2007-1437F and California Geological Survey Special Report 203F.

Dawson, T.E., Weldon, R.J. II, and Biasi, G.P., 2008b, Recurrence interval and event age data for type A faults, appendix B *of* [WGCEP] 2007 Working Group on California Earthquake Probabilities, Uniform California Earthquake Rupture Forecast, version 2 (UCERF2): U.S. Geological Survey Open-File Report 2007-1437B and California Geological Survey Special Report 203B.

Dawson, T.E., McGill, S.F., and Rockwell, T.K., 2003, Irregular recurrence of paleoearthquakes along the central Garlock fault near El Paso Peaks, California: Journal of Geophysical Research, v. 108, doi:10.1029/2001JB001744.

Dolan, J.F., and Rockwell, T.K., 2001, Paleoseismologic evidence for a very large Mw>7 recent surface rupture on the eastern San Cayetano fault, Ventura County, California—Was this the source of the damaging December 21, 1812, earthquake?: Bulletin of the Seismological Society of America*,* v. 91, p. 1417–1432.

Field, E.D., Dawson, T.E., Felzer, K.R., Frankel, A.D., Gupta, V., Jordan, T.H., Parsons, T., Petersen, M.D., Stein, R.S., Weldon, R.J., II, and Wills, C.J., 2009, Uniform California earthquake rupture forecast, version 2 (UCERF 2), Bulletin of the Seismological Society of America, v. 99, p. 2053–2107, doi:10.1785/0120080049.

Field. E.H., Weldon, R.J., II, Gupta, V., Parsons, T., Wills, C.J., Dawson, T.E., Stein, R.S., and Petersen, M.D., 2008, Development of final A-fault rupture models for WGCEP/NSHMP earthquake rate model 2.3, appendix G *of* [WGCEP] 2007 Working Group on California Earthquake Probabilities, contributors, Uniform California Earthquake Rupture Forecast, version 2 (UCERF2): U.S. Geological Survey Open-File Report 2007-1437G and California Geological Survey Special Report 203G.

Fumal, T.E., 2012, Timing of large earthquakes during the past 500 years along the Santa Cruz mountains segment of the San Andreas fault at Mill Canyon, near Watsonville, California: Bulletin of the Seismological Society of America, v. 102, doi:10.1785/0120110161.

Fumal, T.E., Heingarther, G.F., and Schwartz, D.P., 1999, Timing and slip of large earthquakes on the San Andreas fault—Santa Cruz Mountains, California [abs.]: Geological Society of America Abstracts with Programs, v. 31, no. 6, p. A–56.

Fumal, T.E., Weldon, R.J., II, Biasi, G.P., Dawson, T.E., Seitz, G.G., Frost, W., and Schwartz D.P., 2002a, Evidence for large earthquakes on the San Andreas fault at the Wrightwood, California, paleoseismic site—A.D. 500 to present: Bulletin of the Seismological Society of America, v. 92, p. 2726–2760.

Fumal, T.E., Rymer, M.J., and Seitz, G.G., 2002b, Timing of large earthquakes since A.D. 800 on the Mission creek strand of the San Andreas fault zone at Thousand Palms oasis, near Palm Springs, California: Bulletin of the Seismological Society of America, v. 92, no. 7, p. 2841–2860.

Fumal, T.E., Heingartner, G.F., Dawson, T.E., Flowers, R., Hamilton, J.C., Kessler, J., Reidy, L. M., Samrad, L., Seitz, G.G., and Southon, J., 2003, A 100-year average recurrence interval for the San Andreas fault, southern San Francisco bay area, California: Eos (American Geophysical Union Transactions), no. S12B-0388.

Fumal, T.E., Pezzopane, S.K., Weldon R.J., II, and Schwartz. D.P., 1993, A 100-year average recurrence interval for the San Andreas fault at Wrightwood, California: Science, v. 259, p. 199–203.

Ganev, P.N., Dolan, J.F., Blisniuk, K., Oskin, M., and Owen, L., 2010, Paleoseismic evidence for multiple Holocene earthquakes on the Calico fault—Implications for earthquake clustering in the eastern California shear zone: Lithosphere, v. 2, no. 4, p. 287–298, doi:10.1130/L82.1.

Gath, E.M., Gonzalez, T., and Rockwell, T.K., 1992, Slip rate of the Whittier fault based on 3-D trenching at Brea, southern California [abs.]: Geological Society of America Abstracts with Programs, v. 24, no. 5, p. 26.

Goldfinger, C, Morey, A., Nelson, C.H., Gutiérrez-Pastor, J., Johnson, J.E., Karabanov, E., Chaytor, J., Eriksson, A., and the Shipboard Scientific Party, 2007, Rupture lengths and temporal history of significant earthquakes on the offshore and north coast segments of the northern San Andreas fault based on turbidite stratigraphy: Earth and Planetary Science Letters, v. 254, no. 1, p. 9–27.

Grant, L.B., Arrowsmith, J.R., Akciz, S., 2005, A composite chronology of earthquakes from the Bidart Fan paleoseismic site, San Andreas fault, California [abs.]: Eos (American Geophysical Union Transactions), v. 86, Fall meeting supplement, no. 52, abs. U42A-07.

Grant, L.B., Waggoner, J.T., Stein, C.V., and Rockwell T.K., 1997, Paleoseismicity of the north branch of the Newport-Inglewood fault zone in Huntington Beach, California—from cone penetrometer test data: Bulletin Seismological Society America, v. 87, p. 277–293.

Grant, L.B. and Sieh K., 1994, Paleoseismic evidence of clustered earthquakes on the San Andreas fault in the Carrizo plain, California: Journal of Geophysical Research, v. 99, no. B4, p. 6819–6841.

Gurrola, L.D., and Rockwell, T.K., 1996, Timing and slip for prehistoric earthquakes on the Superstition mountain fault, Imperial Valley, southern California: Journal of Geophysical Research, v. 101, no. B3, p. 5977–5985.

Haddad, D.E., Madden, C., Salisbury, J.B., Arrowsmith, J.R., and Weldon, R.J., 2011, LiDAR-derived measurements of slip in the most recent ground-rupturing earthquakes along elements

of the San Andreas fault system [abs.]: Eos (American Geophysical Union Transactions), v. 92, Fall meeting supplement, abs. T31B-2344.

Haddad, D.E., Madden, C., Salisbury, J.B., Arrowsmith, J.R., and Weldon, R.J., 2011, LiDAR-derived measurements of slip in the most recent ground-rupturing earthquakes along elements of the San Andreas fault system [abs.]: Southern California Earthquake Center Annual Meeting Proceedings and Abstracts, Palm Springs, Calif., v. 21, *http://www.scec.org/meetings/2011am/SCECProceedingsXXI-FullVolume.pdf*.

Hayward Fault Paleoearthquake Group (Lienkaemper, J.J., Schwartz, D.P., Kelson, K.I., Lettis, W.R., Simpson, G.D., Southon, J.R., Wanket, J.A., and Williams, P.L.), 1999, Timing of paleoearthquakes on the northern Hayward fault—Preliminary evidence in El Cerrito, California: U.S. Geological Survey Open-File Report, 99–318, 34 p.

Hecker, S., Pantosti, D., Schwartz, D.P., Hamilton, J.C., Reidy, L.M., and Powers, T.J., 2005, The most recent large earthquake on the Rodgers Creek fault, San Francisco bay area: Bulletin of the Seismological Society of America, v. 95, no. 3, p. 844–860.

Hemphill-Haley, M.A., and Witter, R.C., 2006, Latest Pleistocene paleoseismology of the southern Little Salmon Fault, Strong's Creek, Fortuna, California: Final Technical Report, NEHRP Award #04HQGR004, p. 19, *http://www.earthquake.usgs.gov/research/external/%20reports/04HQGR0004.pdf*.

Hemphill-Haley, M.A., and Weldon, R.J. II, 1999, Estimating prehistoric earthquake magnitude from point measurements of surface rupture: Bulletin of the Seismological Society of America, v. 89, p. 1264–1279.

Jing, L.Z., Klinger, Y., Sieh, K., Rubin, C., and Seitz, G., 2006, Serial ruptures of the San Andreas fault, Carrizo plain, California, revealed by three-dimensional excavations: Journal of Geophysical Research, v. 111, no.B2, B02306, doi:10.1029/2004JB003601.

Kelson, K.I., Streig, A.R., Koehler, R.D., 2006, Timing of late Holocene paleoearthquakes on the northern San Andreas fault at the Fort Ross Orchard Site, Sonoma County, California: Bulletin of the Seismological Society of America, v. 96, no. 3, p. 1012–1028.

Kelson, K.I., Simpson, G.D., Lettis, W.R., and Haraden C.C., 1996, Holocene slip rate and recurrence of the northern Calaveras fault at Leyden Creek, northern California: Journal of Geophysical Research, v. 101, no. B3, p. 5961–5975.

Koehler, R.D., Witter, R.C., Simpson, G.D., Hemphill-Haley, E., and Lettis, W.R., 2004, Paleoseismic investigation of the northern San Gregorio fault at Pillar Point marsh near Half Moon Bay, California: U.S. Geological Survey Final Technical Report, Award number 02HQGR0071, *http://earthquake.usgs.gov/research/external/reports/04HQGR0045.pdf*.

Lawson, A.C., 1908, The California earthquake of April 18, 1906—Report of the State Earthquake Investigation Commission: Washington, D.C., Carnegie Institution of Washington Publication 87, 192 p. (Reprinted 1979.)

Leon, L.A., Christofferson, S.A., Dolan, J.F., Shaw, J.H., Pratt, T.L., 2007, Earthquake-by-earthquake fold growth above the Puente Hills blind thrust fault, Los Angeles, California—Implications for fold kinematics and seismic hazard: Journal of Geophysical Research, v. 112, no. B3, doi:10.1029/2006JB004461.

Leon, L.A., Dolan, J.F., Shaw, J.H., Pratt, T.L., 2009, Evidence for large-magnitude Holocene earthquakes on the Compton blind thrust fault, Los Angeles, California: Journal of Geophysical Research, v. 114, no. B12, p. 305, doi:10.1029/2008JB006129.

Lienkaemper J.J., and Williams, P.L., 2007, A record of large earthquakes on the southern Hayward fault for the past 1800 years: Bulletin of the Seismological Society of America, v. 97, p. 1803–1819.

Lienkaemper, J.J., Baker, B., and McFarland, F.S., 2006, Surface slip associated with the 2004 Parkfield, California, earthquake measured on alignment arrays: Bulletin of the Seismological Society of America, v. 96, no. 4B, p. S239–S249.

Lienkaemper, J.J., 2001, 1857 slip on the San Andreas fault southeast of Cholame, California: Bulletin of the Seismological Society of America, v. 91, no. 6, p. 1659–1672, doi:10.1785/0120000043.

Lienkaemper, J.J., Williams, P.L., Dawson, T.E., Personius, S.F., Seitz, G.G., Heller, S., and Schwartz, D.P., 2003, Logs and data from trenches across the Hayward fault at Tyson's Lagoon (Tule Pond), Fremont, Alameda County, California: U.S. Geological Survey Open-File Report 03-488, p. 6, 8 plates, *http://pubs.usgs.gov/of/2003/of03-488/*.

Lienkaemper, J.J., Dawson, T.E., Personius, S.F., Seitz, G.G., Reidy, L.M., and Schwartz, D.P., 2002, A record of large earthquakes on the southern Hayward fault for the past 500 years: Bulletin of the Seismological Society of America, v. 92, p. 2637–2658.

Lienkaemper, J.J., and Prescott, W.H., 1989, Historic surface slip along the San Andreas fault near Parkfield, California: Journal of Geophysical Research, v. 94, no. 17, p. 647–670.

Lienkaemper, J.J., and Sturm, T.A., 1989, Reconstruction of a channel offset in 1857(?) by the San Andreas fault near Cholame, California: Bulletin of the Seismological Society of America, v. 79, p. 901–909.

Lindvall, S.C., Rockwell, T.K., Dawson, T.E., Helms, J.G., and Bowman, K.W., 2002, Evidence for two surface ruptures in the past 500 years on the San Andreas fault at Frazier mountain, California: Bulletin of the Seismological Society of America, v. 92, p. 2689–2703.

Liu, J., Klinger, Y., Sieh, K., and Rubin C., 2004, Six similar sequential ruptures of the San Andreas fault, Carrizo plain, California: Geology, v. 32, no. 8, p. 649–652.

Madden, C.L., Arrowsmith, J.R., Haddad, D.E., Salisbury, J.B., and Weldon, R.J., II, 2011, Compilation of slip in the last earthquake data for high-slip rate faults in California for input into slip dependent rupture forecast [abs.]: Southern California Earthquake Center Annual Meeting Proceedings and Abstracts, Palm Springs, Calif., v. 21, *http://www.scec.org/meetings/2011am/*.

Madden, C.L., Dolan, J.F., Hartleb, R.D., and Gath, E.M., 2005, New paleoseismologic observations from the western Garlock fault—implications for regional fault interactions [abs.]: Eos (American Geophysical Union Transactions), v. 87, Fall Meeting Supplement, abs. T51D-1380.

Madden-Madugo, C.M., Dolan, J.F., and Hartleb, R.G., 2012, New paleoearthquake ages from the western Garlock fault—Implications for regional earthquake occurrence in southern California: Bulletin of the Seismological Society of America, v. 102, p. 2282–2299, doi:10.1785/0120110310.

McAuliffe, L.M., Dolan, J.F., Kirby, E., Haravitch, B., and Alm, S., 2010, Holocene paleoseismology of the southern Panamint valley fault zone—Evaluating seismic clustering along the eastern California shear zone north of the Garlock fault [abs.]: Southern California Earthquake Center Annual Meeting Proceedings and Abstracts, v. 20, p. 249.

McCalpin, J.P., 2009, Paleoseismology (2d ed.): San Diego, Academic Press international geophysics series, v. 95, 613 p.

McGill, S.F., and Rubin, C.M., 1999, Surficial slip distribution on the central Emerson fault during the June 28, 1992, Landers earthquake, California: Journal of Geophysical Research, v. 104, no. B3, p. 4811–4833.

McGill, S.F., Dergham, S., Barton, K., Berney-Ficklin, T., Grant, D., Hartling, C., Hobart, K., Minnich, R., Rodriguez, M., Runnerstrom, E., Russell, J., Schmoker, K., Stumfall, M., Townsend, J., and Williams, J., 2002, Paleoseismology of the San Andreas fault at Plunge Creek, near San Bernardino, southern California: Bulletin of the Seismological Society of America, v. 92, no. 7, p. 2803–2840, doi:10.1785/0120000607.

McGill, S.F., 1992, Paleoseismology and neotectonics of the central and eastern Garlock fault, California: Pasadena, California Institute of Technology, Ph.D. dissertation., 235 p., 8 pl.

McGill, S.F., and Sieh, K., 1991, Surficial offsets on the central and eastern Garlock fault associated with prehistoric earthquakes: Journal of Geophysical Research, v. 96, no. B13, p. 21597–21621.

Middleton, T.J., 2006, Tectonic geomorphology of the southern Clark fault from Anza southeast to the San Felipe Hills: Implications of slip distribution for recent past earthquakes: San Diego State University, M.S. thesis, 109 p.

Niemi, T.M., Zhang, H., Generaux, S., Fumal, T.E., and Seitz, G.G., 2002, A 2500-year record of earthquakes along the northern San Andreas fault at Vedanta Marsh, Olema, California [abs.]: Geological Society of America, Cordilleran Section, Abstracts with Programs, v. 34, no. 5, p. 86.

Noriega, G.R., Arrowsmith, J.R., Grant, L.B., and Young, J.J., 2006, Stream channel offset and late Holocene slip rate of the San Andreas fault at the Van Matre ranch site, Carrizo plain, California: Bulletin of the Seismological Society of America, v. 96, p. 33–47.

Onerdonk, N.W., Rockwell, T.K., McGill, S.F., and Marliyani, G.I., 2013, Evidence for seven surface ruptures in the past 1600 years on the Claremont fault at Mystic Lake, northern San Jacinto fault zone, California: Bulletin of the Seismological Society of America, v. 103, no. 1, p. 519–541, doi:10.1785/0120120060.

Padgett, D.C., 1994, Paleoseismology of the Lenwood fault, Mojave Desert, San Bernardino County, California: Los Angeles, California State University, M.S. thesis, 90 p.

Patterson, A.C., and Rockwell, T.K., 1993, Paleoseismology of the Whittier fault based on 3-dimensional trenching at Olinda oil field, Orange County, southern California [abs.]: Geological Society of America Abstracts with Programs, v. 25, no. 5, p. 131.

Peterson, M.D., Dawson, T.E., Chen, R., Tianqing, C., Wills, C.J., Schwarz, D.P., and Frankel, A.D., 2011, Fault displacement hazard for strike slip faults: Bulletin of the Seismological Society of America, v. 101, no. 2, p. 805–825, doi:10.1785/0120100035.

Philibosian, B., Fumal, T.E., and Weldon, R.J., II, 2011, San Andreas fault earthquake chronology and Lake Cahuilla history at Coachella, California: Bulletin of the Seismological Society of America, v. 101, doi:10.1785/0120100050.

Philibosian, B., Fumal, T., Kendrick, K., Weldon, R., Scharer, K., Bemis, S., Burgette, R., and Wisely, B., 2009, Photomosaics and logs of trenches on the San Andreas fault near Coachella, California: U.S. Geological Survey Open-File Report 2009–1039.

Philibosian, B., Fumal, T., Kendrick, K., and Weldon, R.J., II, 2006, Paleoseismic investigation of the San Andreas fault at Coachella, California [abs.]: Eos (American Geophysical Union Transactions), v. 87, Fall meeting supplement, abs. T21C-0438.

Prentice, C.S., and Ponti, D.J., 1997, Coseismic deformation of the Wrights tunnel during the 1906 San Francisco earthquake—A key to understanding 1906 fault slip and 1989 surface

ruptures in the southern Santa Cruz Mountains, California: Journal Geophysical Research, v. 102, no. B1, p. 635–648.
Ramzan S., and Yule J.D., 2011, Paleoseismic investigation of the San Gorgonio Pass fault zone near Cabezon, California [abs.]: Southern California Earthquake Center Annual Meeting Proceedings and Abstracts, Palm Springs, Calif., v. 21, *http://www.scec.org/meetings/2011am/*.
Rockwell, T., Seitz, G., Dawson, T., and Young, J., 2006, The long record of San Jacinto fault paleoearthquakes at Hog Lake—Implications for regional patterns of strain release in the southern San Andreas fault system [abs.]: Seismological Research Letters, v. 77, p. 270.
Rockwell, T.K., McElwain, R.S., Millman, D.E., and Lamar, D.L., 1986, Recurrent late Holocene faulting on the Glen Ivy north strand of the Elsinore fault at Glen Ivy marsh, *in* Ehlig, P.L., ed., Neotectonics and faulting in southern California: Geological Society of America, Cordilleran Section, Guidebook and Volume, p. 167–175.
Rubin, C.M., Lindvall, S.C., and Rockwell, T.K., 1998, Evidence for large earthquakes in metropolitan Los Angeles: Science, v. 281, no. 5375, p. 398–402.
Runnerstrom, E.E., Grant, L.B., Arrowsmith, J.R., Rhodes, D.D., and Stone, E.M., 2002, Displacement across the Cholame segment of the San Andreas fault between 1855 and 1893 from Cadastral Surveys: Bulletin of the Seismological Society of America, v. 92, no. 7, p. 2659–2669.
Rust, D.J., 1986, Neotectonic behavior of the San Andreas zone in the Big Bend [abs.]: Geological Society of America Abstracts with Programs, v. 18, p. 177.
Rust, D.J., 1982, Radiocarbon dates for the most recent large prehistoric earthquakes and late Holocene slip rates—San Andreas fault in part of the Transverse Ranges north of Los Angeles [abs.]: Geological Society of America Abstracts with Programs, v. 14, p. 229.
Rymer, M.J., Tinsley, J.C., III, Treiman, J.A., Arrowsmith, J R., Clahan, K.B., Rosinski, A.M., Bryant, W.A., Snyder, H.A., Fuis, G.S., Toké N.A., and Bawden, G.W., 2006, Surface fault slip associated with the 2004 Parkfield, California, Earthquake: Bulletin of the Seismological Society of America, v. 96, p. 11–27.
Salisbury, J.B., Rockwell, T.K., Middleton, T.J., and Hudnut K.W., 2012, LiDAR and field observations of slip distribution for the most recent surface ruptures along the central San Jacinto fault: Bulletin of the Seismological Society of America, v. 102, no. 2, p. 598–619, doi:10.1785/0120110068.
Salyards, S.L., Sieh, K.E., and Kirschvink, J.L., 1992, Paleomagnetic measurement of non-brittle coseismic deformation across the San Andreas fault at Pallett Creek, California: Journal of Geophysical Research, v. 96, no. B9, p. 12457–12470.
Scharer, K.M., Biasi, G.P., and Weldon, R.J., II, 2011, A re-evaluation of the Pallett Creek earthquake chronology based on new AMS radiocarbon dates, San Andreas fault, California: Journal Geophysical Research, doi:10.1029/2010JB008099.
Scharer, K.M., Biasi, G.P., Weldon, R.J., II, and Fumal, T.E., 2010, Quasi-periodic recurrence of large earthquakes on the southern San Andreas fault: Geology, v. 38, no. 6, p. 555–558.
Scharer, K.M., 2010, Changing views of the San Andreas fault: Science, v. 327, p. 1089–1090, doi:10.1126/science.1186770.
Scharer, K.M., Weldon, R.J., II, Fumal, T.E., and Biasi, G.P., 2007, Paleoearthquakes on the southern San Andreas fault, Wrightwood, California, 3000 to 1500 B.C.—A new method for evaluating paleoseismic evidence and earthquake horizons: Bulletin of the Seismological Society of America, v. 97, no. 4, p. 1054–1093.

Schwartz, D.P., Pantosti, D., Hecker, S., Okumura, K., Budding, K.E., and Powers, T., 1992, Late Holocene behavior and seismogenic potential of the Rodgers Creek fault zone, Sonoma County, California *in* Borchardt, G., Hirschfeld, S.E., Lienkaemper, J.J., McClellan, P., and Wong, I.G., eds., Proceedings of the second conference on earthquake hazards in the eastern San Francisco Bay area: California Division of Mines and Geology, Special Publication 113, p. 393–398.

Seitz, G., Kent, G., Smith, S., Dingler, J., Driscoll, N., Karlin, R., Babcock, J., and Harding, A., 2006, Multi-method paleoseismology—combining on and offshore data to build a basin wide record of earthquakes at Lake Tahoe [abs.]: Seismological Research Letters, v. 77, no. 2, Seismological Society of America 100th anniversary earthquake conference and annual meeting, p. 274.

Seitz G.G., Kent, G., 2004, Closing the gap between on and offshore paleoseismic records in the Lake Tahoe basin: U.S. Geological Survey Final Technical Report, National Earthquake Hazards Reduction Program, External Grant Award Number 04HQGR007, 14 p., *http://earthquake.usgs.gov/research/external/reports/04HQGR0017.pdf/*.

Seitz, G., Biasi, G., and Weldon, R.J., II, 2000, An improved paleoseismic record of the San Andreas fault at Pitman canyon *in* Noller, J.S., Sowers, J.M., and Lettis, W.R., eds., Quaternary geochronology—Methods and applications: Washington, D.C., American Geophysical Union Ref. Shelf 4, vol. 4, p. 563–566, doi:10.1029/RF004p0563.

Seitz, G.G., 1999, The paleoseismology of the San Andreas fault at Pitman canyon—Implication for fault behavior and paleoseismic methodology: Eugene, University of Oregon, Ph.D. Dissertation, 278 p.

Seitz, G., Weldon, R.J., II, and Biasi, G., 1996, The Pitman canyon paleoseismic record—A re-evaluation of San Andreas fault segmentation: Journal of Geodynamics, v. 24, p. 129–138.

Seitz, G., and Weldon, R., 1994, The paleoseismology of the southern San Andreas fault at Pitman canyon, San Bernardino, California in McGill, S.F., and Ross, T.M., eds., Geological Investigations of an Active Margin, Geological Society of America Cordilleran Section Guidebook, trip 8, p. 152–156.

Sickler, R., Weldon, R., Fumal, T., Schwartz, D., Mezger, L., Alexander, J., Biasi, G., Burgette, R., Goldman, M., Saldana, S., 2006, Slip rate of the San Andreas fault near Littlerock, California: Seismological Research Letters, v. 77, no. 2, p. 250–251.

Sieh, K., Jones, L., Hauksson, E., Hudnut, K., Eberhart, P., Heaton, T., Hough, T., Hutton, L., Kanamori, H., Lilje, A., Lindvall, S., McGill, S., Mori, J., Rubin, C., Spotila, J., Stock, J., Thio, H., Treiman, J., Wernicke, B., and Zachariasen, J., 1993, Near-field investigations of the Landers earthquake sequence, April to July 1992: Science, v. 260, p. 171–176.

Sieh, K.E., Stuiver, M., and Brillinger, D., 1989, A more precise chronology of earthquakes produced by the San Andreas fault in southern California: Journal of Geophysical Research, v. 94, no. B1, p. 603–623.

Sieh, K.E., 1986, Slip rate across the San Andreas fault and prehistoric earthquakes at Indio, California [abs.]: Eos (American Geophysical Union Transactions), v. 67, no. 44, p. 1200, Fall meeting supplement, abs. T22C-01.

Sieh, K.E., 1984, Lateral offset and revised dates of large prehistoric earthquakes at Pallett Creek, southern California: Journal of Geophysical Research, v. 89, p. 7641–7670.

Sieh, K.E., 1978, Prehistoric large earthquakes produced by slip on the San Andreas fault at Pallett Creek, California: Journal of Geophysical Research, v. 83, no. B8, p. 3907–3939.

Sieh, K. E., 1978, Slip along the San Andreas fault associated with the great 1857 earthquake: Bulletin of the Seismological Society of America, v. 68, no. 5, p.1421–1448.

Simpson, G.D., Baldwin, J.N., Kelson, K.I., and Lettis, W.R., 1999, Late Holocene slip rate and earthquake history for the northern Calaveras fault at Welch Creek, eastern San Francisco Bay area, California: Bulletin of the Seismological Society of America, v. 89, no. 5, p. 1250–1263.

Simpson, G.D., Thompson, S.C., Noller, J.S., and Lettis, W.R., 1997, The northern San Gregorio fault zone—Evidence for timing of late Holocene earthquakes near Seal Cove, California: Bulletin of the Seismological Society of America, v. 87, no. 5, p. 1158–1170.

Simpson, G.D., Noller, J.S., Kelson, K.I., and Lettis W.R., 1996, Log of trenches across the San Andreas fault, Archea Camp, Fort Ross Historic Park, Northern California: U.S. Geological Survey Final Technical Report, National Earthquake Hazards Reduction Program, Award Number 1434-94-G-2474.

Sims, J.D., 1994, Stream channel offset and abandonment and a 200-year average recurrence interval of earthquakes on the San Andreas fault at Phelan Creek, Carrizo plain, California *in* Schwartz, D.P., and Yeats, R.S., eds., Proceedings of the workshop on paleoseismology, 18–22 September 1994, Marshall, California: U.S. Geological Survey Open-File Report 94-568, p. 170–172.

Sims, J.D., Ito, T., Hamilton, J.C., and Meier, D.B., 1989, Late Holocene record of earthquakes and slip along the San Andreas fault in excavations on the Carrizo plain, central California [abs.]: Eos (American Geophysical Union Transactions), v. 70, p. 1349, Fall meeting supplement.

Stone, E.M., 2002, Recent rupture history of the San Andreas fault southeast of Cholame in the northern Carrizo plain, California: Bulletin of the Seismological Society of America, v. 92, no. 3, p. 983–997.

Streig, A.R., Dawson, T.E., and Weldon, R.J. II, in press, Surface rupturing earthquakes on the Santa Cruz mountains section of the San Andreas fault, near Corralitos, CA—Paleoseismic evidence of the 24 April 1890 and June 1838 earthquakes?: Bulletin of the Seismological Society of America.

Thatcher, W., Marshall, G., and Lisowski, M, 1997, Resolution of fault slip along the 470-km-long rupture of the great 1906 San Francisco earthquake and its implications: Journal of Geophysical Research, v. 102, no. B3, p. 5353–5367.

Thorup, K.M., 1997, Paleoseismology of the central Elsinore fault in southern California—Results from three trench sites: San Diego, Calif., San Diego State University, M.S. thesis, 94 p.

Toke, N.A., and Arrowsmith, J.R., 2006, Reassessment of a slip budget along the Parkfield segment of the San Andreas fault: Bulletin of the Seismological Society of America, v. 96, no. 4, p. S1–S, doi:10.1785/0120050829.

Toppozada, T.R., Branum, D.M., Reichle, M.S., and Hallstrom, C.L., 2002, San Andreas fault zone, California—M>5.5 earthquake history: Bulletin of the Seismological Society of America, v. 92, no. 7, p. 2555–2601.

Toppozada, T.R., Real, C.B., and Parke, D.L., 1981, Preparation of isoseismal maps and summaries of reported effects for pre-1900 California earthquakes: Sacramento, Calif., California Division of Mines and Geology Open-File Report 81-11 SAC.

Tucker, A.Z., Dolan, J.F., 2001, Paleoseismologic evidence for a >8 ka age for the most recent surface rupture on the eastern Sierra Madre fault, northern Los Angeles metropolitan region: Bulletin of the Seismological Society of America, v. 91, p. 232–249.

Vaughan, P.R., Thorup, K.M., and Rockwell, T.K., 1999, Paleoseismology of the Elsinore fault at Agua Tibia mountain, southern California: Bulletin of the Seismological Society of America, v. 89, no. 6, p. 1447–1457.

Walls, C., and Gath, E.M., 2001, Tectonic geomorphology and Holocene surface rupture on the Chino fault, southern California [abs.]: Southern California Earthquake Center Annual Meeting Proceedings and Abstracts, v. 11, p. 118.

Weldon, R.J., II, and Scharer, K., 2009, Slip rates for the San Andreas fault between the Big Bend and the San Bernardino valley, southern California: U.S. Geological Survey Final Technical Report, National Earthquake Hazards Reduction Program, 10 p.

Weldon, R.J., II, Biasi, G.P., Wills, C.J., and Dawson, T.E., 2008, Overview of the southern San Andreas fault model, appendix E *of* [WGCEP] 2007 Working Group on California Earthquake Probabilities, contributors, Uniform California Earthquake Rupture Forecast, version 2 (UCERF2): U.S. Geological Survey Open-File Report 2007-1437E and California Geological Survey Special Report 203E.

Weldon, R.J., II, Fumal, T.E., Biasi, G.P., and Scharer, K.M., 2005, Past and future earthquakes on the San Andreas fault: Science, v. 308, p. 966–967.

Weldon, R.J, II, Scharer, K., Fumal, T., and Biasi, G., 2004, Wrightwood and the earthquake cycle—what the long recurrence record tells us about how faults work: GSA Today, v. 14, p. 4–10, doi:10.1130/1052-5173(2004)014.

Weldon, R.J., II, Fumal, T.E., Powers, T., Pezzopane, S.K., Scharer, K.M., and Hamilton, J.C., 2002, Structure and earthquake offsets on the San Andreas fault at the Wrightwood, California paleoseismic site: Bulletin of the Seismological Society of America, v. 92, no. 7, p. 2704–2725.

Weldon, R.J., II, and Sieh, K.E., 1985, Holocene rate of slip and tentative recurrence interval for large earthquakes on the San Andreas fault, Cajon Pass, southern California: Geological Society of America Bulletin, v. 96, no. 6, p. 793–812.

Wells, D.L., and Coppersmith, K.J., 1994, New empirical relationships among magnitude, rupture length, rupture width, rupture area, and surface displacement: Bulletin of the Seismological Society of America, v. 84, no. 4, p. 974–1002.

Wells, D.L., and Coppersmith, K.L., 1993, Likelihood of surface rupture as a function of magnitude [abs.]: Seismological Research Letters, v. 64, no. 1, p. 54.

Wesnousky, S.G., 2008, Displacement and geometrical characteristics of earthquake surface ruptures—issues and implications for seismic-hazard analysis and the process of earthquake rupture: Bulletin of the Seismological Society of America, v. 98, p. 1609–1632.

Williams, P.L., and Seitz, G.G., 2005 San Andreas fault in the Coachella Valley at Salt Creek—development of long term earthquake chronology and event offsets [abs.]: Southern California Earthquake Center, annual meeting, proceedings and abstracts, v. 14.

Wills, C.J., Weldon, R.J. II, and Bryant, W.A., 2008, California fault parameters for the National Seismic Hazard Map and Working Group on California Earthquake Probabilities 2007—Appendix A *of* (WGCEP) 2007 Working Group on California Earthquake Probabilities, Uniform California Earthquake Rupture Forecast, version 2 (UCERF2): U.S. Geological Survey Open-File Report 2007–1437A and California Geological Survey Special Report 203A.

Wills, C.J., Weldon, R.J. II, and Field, E.H., 2008, A-Priori rupture models for northern California Type-A faults—Appendix K *of* (WGCEP) 2007 Working Group on California Earthquake Probabilities, Uniform California Earthquake Rupture Forecast, version 2

(UCERF2): U.S. Geological Survey Open-File Report 2007–1437K and California Geological Survey Special Report 203K.

Working Group on California Earthquake Probabilities [WGCEP], 2008, The uniform California earthquake rupture forecast—version 2 (UCERF 2): U.S. Geological Survey Open-File Report 2007–1437 and California Geological Survey Special Report 203.

Working Group on California Earthquake Probabilities [WGCEP], 2003, Earthquake probabilities in the San Francisco Bay region—2002–2031: U.S. Geological Survey Open-File Report 2003–214, 253 p., *http://pubs.usgs.gov/of/2003/of03-214/*.

Working Group on California Earthquake Probabilities [WGCEP], 1990, Probabilities of large earthquakes in the San Francisco Bay Region, California: U.S. Geological Survey Circular 1053, 51 p., *http://pubs.er.usgs.gov/publication/cir1053/*.

Working Group on California Earthquake Probabilities [WGCEP], 1999, Earthquake Probabilities in the San Francisco Bay Region—2000–2030—a summary of findings: U.S. Geological Survey Open-File Report 99–517, Online Version 1.0, 36 p.

Working Group on California Earthquake Probabilities [WGCEP], Jackson, D.D., Aki, K., Cornell, C.A., Dieterich, J.H., Henyey, T.L., Mahdyiar, M., Schwartz, D., and Ward, S.N., 1995, Seismic hazards in southern California—probable earthquakes, 1994–2024: Bulletin of the Seismological Society of America, v. 85, p. 379–439.

Working Group on California Earthquake Probabilities [WGCEP], 1988, Probabilities of large earthquakes occurring in California on the San Andreas fault system: U.S. Geological Survey Open-File Report 88–398, 62 p.

Young, J.J., Arrowsmith, J.R., Colini, L., and Grant L.B., 2002, 3 dimensional excavation and measurement of recent rupture history along the Cholame segment of the San Andreas fault: Bulletin of the Seismological Society of America, v. 92, p. 2670–2688.

Yu, E., and Segall, P., 1996, Slip in the 1868 Hayward earthquake from the analysis of historical triangulation data: Journal of Geophysical Research, v. 101, no. B7, p. 16101–16118.

Yule, J.D., and McBurnett, P.L., 2011, Paleoseismology and slip rate of the San Gorgonio pass fault zone at Millard canyon—Testing the likelihood of through-going San Andreas ruptures [abs.]: Southern California Earthquake Center Annual Meeting Proceedings and Abstracts, v. 21, p. 258, *http://www.scec.org/meetings/2011am/*.

Yule, D., Maloney, S., and Cummings, L.S., 2006, Using pollen to constrain the age of the youngest rupture of the San Andreas fault at San Gorgonio pass [abs.]: 2006 Annual Meeting, Seismological Society of America, San Francisco, Calif., 100th Anniversary Earthquake Conference, Seismological Research Letters, v. 77, no. 2, p. 245.

Yule, D., and Sieh, K., 2001, The paleoseismic record at Burro Flats—evidence for a 300-year average recurrence of large earthquakes on the San Andreas fault in San Gorgonio Pass, southern California, Cordilleran Section [abs.]: American Association of Petroleum Geologists, Pacific section annual meeting, April 9–11, *https://gsa.confex.com/gsa/2001CD/finalprogram/abstract_4270.htm*.

Zhang, H., 2006, Paleoseismic studies of the northern San Andreas fault at Vedanta marsh site, Olema, California: Kansas City, University of Missouri, Ph.D. dissertation, 334 p.

Zhang, H., Niemi, T., and Fumal T., 2006, A 3000-year record of earthquakes on the northern San Andreas fault at the Vedanta marsh site, Olema, California [abs.]: 2006 Annual Meeting, Seismological Society of America, San Francisco, Calif., 100th Anniversary Earthquake Conference: Seismological Research Letters, v. 77, no. 2, p. 176.

Zhang, H., Niemi, T.M., Generaux, S., Fumal, T.E., 2003a, Earthquake events and recurrence interval on the northern San Andreas fault at Vedanta marsh site, Olema, CA [abs.]: Geological Society of America, north-central section, 37th annual meeting, Abstracts with Programs, v. 35, no. 2, p. 58.

Zhang, H., Niemi, T.M., Generaux, S., Fumal, T.E., and Seitz, G.G., 2003b, Paleoseismology of the northern San Andreas fault at Vedanta Marsh site, Olema, California [abs.]: Congress of the International Union for Quaternary Research, 16th INQUA congress, Shaping the Earth—a Quaternary perspective, v. 16, p. 107.

Zhang, P., Ellis, M., Slemmons, D.B., and Mao, F., 1990, Right-lateral displacements and the Holocene slip rate associated with prehistoric earthquakes along the southern Panamint Valley fault zone—Implications for southern basin and range tectonics and coastal California deformation: Journal Geophysical Research, v. 95, no. B4, p. 4857–4872.

Zielke, O., Arrowsmith, J.R., Grant Ludwig, L., Akçiz, S.O., 2012, High-resolution topography-derived offsets along the 1857 Fort Tejon earthquake rupture trace, San Andreas fault: Bulletin of the Seismological Society of America, v. 102, p. 1135–1154.

Zielke, O., Arrowsmith, J.R., Grant-Ludwig, L.B., and Akciz, S.O., 2010, Slip in the 1857 and earlier large earthquakes along the Carrizo segment, San Andreas fault: Science, v. 327, p. 1119–1121.

Table G1. Paleoseismic sites used in Uniform California Earthquake Rupture Forecast, version 3 (UCERF3).

UCERF3 Fault Section	Site	Comments	Reference
Calaveras (No) 2011 CFM	Welch/Leyden Creeks	Used in UCERF2	Kelson and others (1996), Simpson and others (1999)
Compton	Stanford Ave	New site	Leon and others (2009)
Elsinore (Coyote Mountains)	Coyote Mts	New site	Rockwell and others (1986)
Elsinore (Glen Ivy) rev	Glen Ivy	Used in UCERF2	Rockwell and others (1986); Rockwell (written communication, 2007); Dawson and others (2008)
Elsinore (Julian)	Lake Henshaw	New site	Thorup (1997)
Elsinore (Julian)	Julian	Used in UCERF2	Thorup (1997)
Elsinore (Temecula)	Temecula	Used in UCERF2	Vaughan and others (1999)
Garlock (Central)	El Paso Peaks	Used in UCERF2	Dawson and others (2003)
Garlock (Central)	Central Searles	New site	McGill (1992)
Garlock (Western)	Twin Lakes	Used in UCERF2	Madden-Madugo and others (2012); Madden and Dolan (2004)
Green Valley 2011 CFM	Lopes Ranch	New site	Lienkaemper and others, submitted to BSSA 3/1/2012
Green Valley 2011 CFM	Mason Road	New site	Lienkaemper and others, submitted to BSSA 2/1/2012
Hayward (No) 2011 CFM	Mira Vista	Used in UCERF2	HPEG (1999); Dawson and others (2008)
Hayward (So) 2011 CFM	Tule Pond	Revised	Lienkaemper and others (2010)
Little Salmon (Onshore)	College of the Redwoods	New site	Carver and Burke (1988)
Little Salmon (Onshore)	Little Salmon Creek	New site	Carver and Burke (1988)
North Frontal (West)	Marble Canyon	New site	Anderson (2002)
North Tahoe 2011 CFM	North Tahoe Basin	New site	Smith and others (2013); Brothers and others (2009); Seitz and others (2006); Seitz and others (2004).
Panamint Valley	Goler Wash	New site	McAuliffe and others (2010)

UCERF3 Fault Section	Site	Comments	Reference
Puente Hills	Santa Fe Springs	New site	Dolan and others (2003)
Rodgers Creek-Healdsburg 2011 CFM	Triangle G	New site	Budding and others (1991); Hecker and others (2005)
Rodgers Creek-Healdsburg 2011 CFM	Triangle G	Used in UCERF2	Budding and others (1991); Hecker and others (2005); Schwartz and others (1992)
San Andreas (Big Bend)	Frazier	New site	Scharer and others, Unpublished data
San Andreas (Carrizo)	Bidart	Revised	Akçiz and others (2009)
San Andreas (Coachella)	Coachella	New site	Philibosian and others (2011)
San Andreas (Coachella)	Indio	Used in UCERF2	Sieh (1986)
San Andreas (Coachella)	Thousand Palms	Used in UCERF2	Fumal and others (2002)
San Andreas (Mojave S)	Pallett Creek	Revised	Scharer and others (2011)
San Andreas (Mojave S)	Wrightwood deep	Revised	
San Andreas (Mojave S)	Wrightwood deep	New, deeper section	Scharer and others (2007)
San Andreas (North Coast) 2011 CFM	Alder Creek	New site	Baldwin (1996)
San Andreas (North Coast) 2011 CFM	Vendanta	Used in UCERF2	Zhang and others (2006); Zhang and others (2005); Zhang and others (2003a); Zhang and others (2003b); Niemi and others (2002)
San Andreas (Offshore) 2011 CFM	Offshore	Used in UCERF3	Goldfinger and others (2007)
San Andreas (Peninsula) 2011 CFM	Filoli	New site	Hall and others (1999)
San Andreas (San Bernardino N)	Pitman Canyon	Revised	Seitz and others (1996); Seitz and others (2000)
San Andreas (San Bernardino N)	Plunge Creek	Used in UCERF2	McGill and others (2002)
San Andreas (San Bernardino S)	Burro Flat	Used in UCERF2	Yule and Sieh (2001); Yule and others (2006)
San Andreas (Santa Cruz Mountains) 2011 CFM	Arano	Revised	Fumal (written communication, 2007); Dawson and others (2008).
San Andreas (Santa Cruz Mountains) 2011 CFM	Hazel Dell	New	Streig and others (2013)
San Andreas (Santa Cruz Mountains) 2011 CFM	Mill Canyon	Revised	Fumal (2012)

UCERF3 Fault Section	Site	Comments	Reference
San Cayetano	Piru	New site	Dolan and Rockwell (2001)
San Gorgonio Pass	Cabazon	New site	Ramzan and Yule (2011)
San Gregorio (North) 2011 CFM	Seal Cove	Revised	Simpson and others (1997)
San Jacinto (Anza)	Blackburn Canyon	New site	Salisbury and others, 2012; Buga and others, 2011
San Jacinto (Anza)	Hog Lake	Used in UCERF2	Rockwell and others (2006); Rockwell (personal communication, 2013); Dawson and others (2008)
San Jacinto (Claremont)	Mystic Lake	New site – added during review, not used for RI in UCERF 3	Onerdonk and others (2013)
San Jacinto (Clark)	Lute Ridge	New site	Salisbury and others (2012)
San Jacinto (Superstition Mtn)	Superstition Mt	Used in UCERF2	Gurrola and Rockwell (1996)
Sierra Madre	San Dimas	New site	Tucker and Dolan (2001)
Whittier	Whittier	Used in UCERF2	Patterson and Rockwell (1993); Tom Rockwell (written communication, 2007)

Table G2. Paleoseismic event ages and intervals used in the uniform California earthquake rupture forecast, version 3 (UCERF3).

[Standard error=sqrt(var(x)); RI, recurrence interval; MRE, most recent event; bp, before present (where present is 1950)]

Calaveras (North)				**Latitude: 37.51039**		**Longitude: -121.8346**
			Welch/Leyden Creeks			
Event	**Calendar age (calibrated 2-sigma)**	**AD, unless noted otherwise**	**Interval ID**	**Min interval (years)**	**Max interval (years)**	**Mid ("preferred")**
	Old	Young				
			OPEN	581	846	713.5
Y	1160	1425				
			I1	0	1015	507.5
X	410	1280				
			I2	0	1148	574
W	132	640				
			I3	0	1160	580
V (old is BC)	520*	380				
			I4	0	unconstrained	
U	unconstrained	0*				

RI (time/intervals method)						
Time max (years)	**Time min (years)**	**Intervals**	**Intervals max**	**RI max (years)**	**RI min (years)**	**RI preferred (years)**
2381	1861	4	5	595	372	484

*Constraining dates: 520 BC to 0.

Note: Published RI 250–800 years (Kelson used different method); MRE a combo of published data. Low bound from Kelson and others, 1996; upper constraint from Simpson and others, 1999. This was used in WGCEP 2003.

Other event ages from Leyden Creek site (Kelson and others, 1996).

Compton **Latitude: 33.965991** **Longitude: -118.262921**

Stanford Avenue

Event	Thousands of years before present (ka)	Thousands of years before present (ka)	preferred	Interval ID	Min interval (ka)	Max interval (ka)	Mid ("preferred")
	Old	Young					
				OPEN	0.7	1.75	1.225
Event 1	1.75	0.7					
				I1	0	2.7	
Event 2	3.4	0.7 or 1.9					
				I2	2.2	6.5	
Event 3	7.2	5.6					
				I3	0	2.8	1.4
Event 4	8.4	5.4					
				I4	1.9	7.1	4.5
Event 5	12.5	10.3					
				I5	0	3.4	1.7
Event 6	13.7	10.3					

RI (time/intervals method)

Time max (years)	Time min (years)	Intervals	RI max (years)	RI min (years)	RI preferred (years)
13,000	8,550	5	2,600	1,710	2,155

Note: Grant and others (1997) conducted cone penetrometer testing (CPT) across the Newport-Inglewood fault and find that the Newport-Inglewood fault has the same event history as the Compton fault (Grant and others, 1997).

Elsinore (Coyote Mountains)

No constrained event ages for Coyote Mountains.

Open interval: ~100 years (fault may have ruptured during Laguna Salada earthquake?)

3 events in 2,000 years

Elsinore (Glen Ivy) **Latitude: 33.7701** **Longitude: -117.4909**

Glen Ivy

Event	Calendar age range (calibrated 2-sigma)	AD, unless noted otherwise	Interval	Min interval (years)	Max interval (years)	Mid ("preferred")
	Old	Young				
			OPEN	96	96	96
E1	1910	1910				
			I1	53	283	168
E2	1627	1857				
			I2	39	417	228
E3	1440	1588				
			I3	21	305	163
E4	1283	1419				
			I4	0	189	94.5
E5	1230	1290				
			I5	114	327	220.5
E6	963	1116				

RI (time/intervals method)

Time max (years)	Time min (years)	Intervals	RI max (years)	RI min (years)	RI preferred (years)
947	794	5	189	159	174

Elsinore (Julian) **Latitude: 33.2071** **Longitude: -116.7273**

Julian

Event	Age (years bp)	Age (years bp)	Interval	Min interval (years)	Max interval (years)	Mid (aka "preferred")
			OPEN	1500	2000	1750
MRE	1500	2000				
			I1	1000	2000	1500
PEN	3000	3500				

Elsinore (Julian)—Continued.

RI (time/intervals method)					
Time max (years)	Time min (yrs)	Intervals	RI max (yrs)	RI min (yrs)	RI preferred (years)
2000	1000	1	2000	1000	1500

Elsinore Fault (Julian)

Latitude: 33.35683 Longitude: -117.0097

Lake Henshaw

Event	Age (years bp)	Age (years bp)	Interval	Min interval (years)	Max interval (years)	Mid ("preferred")
			OPEN	700	1700	1200
MRE	1700	700				

Elsinore (Temecula)

Latitude: 33.41 Longitude: -117.04

Temecula

Event	Age in calendar years for MRE (calibrated 2-sigma)	Age in calendar years for MRE (calibrated 2-sigma)	Interval	Min interval (years)	Max interval (years)	Mid ("preferred")
X	1655	1810	**OPEN**	196	351	273.5
Incomplete record until Event T						
	In years bp, below					
	Young	**Old**				
Event T	2700	3300				
			I1	0	800	400
Event P	3000	3500				
			I2	0	1500	750
Event L	3500	4500				
			I3	500	Unconstrained	Unconstrained
*Event H	4500	>4500				

Elsinore (Temecula)—Continued.

RI (time/intervals method)					
Time max (years)	Time min (years)	Intervals	RI max (years)	RI min (years)	RI preferred (years)
>1800	1200	3	>600	400	500

*Event H reported as shortly before 4,500 years. Can use this as a minimum recurrence interval between L and H.

Garlock (Central)

Latitude: 35.4441 **Longitude: -117.6815**

El Paso Peaks

Event	Calendar age (calibrated 2-sigma)	AD unless noted otherwise	Interval ID	Min interval (years)	Max interval (years)	Mid ("preferred")
	Old	Young				
			OPEN	366	556	461
E1	1450	1640				
			I1	500	965	732.5
E2	675	950				
			I2	200	700	450
E3	250	475				
			I3	0	450	225
E4	25	275				
			I4	2955	3615	3285
E5 (yrs in BC)	3340	2930				
			I5	1330	2070	1700
E6 (yrs in BC)	5000	4670				

RI (time/intervals method)					
Time max (years)	Time min (years)	Intervals	RI max (years)	RI min (years)	RI preferred (years)
6640	6120	5	1328	1224	1276

Note: Event ages from Dawson and others (2003).

Garlock (Central) | **Latitude: 35.523424** | **Longitude: -117.372841** | **Searles Valley**

Event	Calendar age (calibrated 2-sigma)	AD unless noted otherwise	Interval ID	Min interval (years)	Max interval (years)	Mid ("preferred")
	Old	Young				
			OPEN		522	
MRE	1490					

Garlock (Western) | **Latitude: 34.9868** | **Longitude: -118.508** | **Twin Lakes**

Event	Calendar age (calibrated 2-sigma)	AD unless noted otherwise	Interval ID	Min interval (years)	Max interval (years)	Mid ("preferred")
	Old	Young				
			OPEN	156	486	321
Event A	1520	1850				
			I1	0	1250	625
Event C	600	1550				
			I2	0	1390	695
Event E	160	620				
			I3	2260	3920	3090
Event I (yrs in BC)	3300	2100				
			I4	0	1400	700
Event K (yrs in BC)	3500	2400				

RI (time/intervals method)

Time max (yrs)	Time min (years)	Intervals	RI max (years)	RI min (years)	RI preferred (years)
5350	3920	4	1338	980	1159

*Time determined by oldest constraining date.

Green Valley **Latitude: 38.132456** **Longitude: -122.122902**

Lopes Ranch

Event	Calendar age (calibrated 2-sigma)	AD unless noted otherwise	Preferred	Interval ID	Min interval (years)	Max interval (years)	Mid ("preferred")
	Old	Young					
				OPEN	291	502	403
E1	1510	1721	1609				
				I1	1188	1574	1371
E2	147	322	238				
				I2	93	413	256
E3	-91	54	-18				

RI (time/intervals method)

Time max	Time min (years)	Intervals	RI max (years)	RI min (years)	RI preferred (years)
1,812	1,456	2	906	728	817

Green Valley **Latitude: 38.240934** **Longitude: -122.163795**

Mason Road

Event	Calendar age (calibrated 2-sigma)	AD unless noted otherwise	Preferred	Interval ID	Min interval (years)	Max interval (years)	Mid ("preferred")
	Old	Young					
				OPEN	240	573	407
E1	1439	1772	1605				
				I1	24	527	280
E2	1245	1415	1325				
				I2	40	295	161
E3	1120	1205	1164				
				I3	45	278	151
E4	927	1075	1013				

RI (time/intervals method)

Time max (years)	Time min (years)	Intervals	RI max (years)	RI min (years)	RI preferred (years)
845	364	3	282	121	201

Hayward (North) **Latitude: 37.9306** **Longitude: -122.2977**

Mira Vista

Event	Calendar age (calibrated 2-sigma)	AD unless noted otherwise	Interval ID	Min interval (years)	Max interval (years)	Mid ("preferred")
	Old	Young				
			OPEN	230	356	293
E1	1650	1776				
			I1	220	706	463
E2	1070	1430				
			I2	120	610	365
E3	820	950				
			I3	30	420	225
E4	530	790				
			I4	0	690	345
E5	100	650				
			I5	0	700	350
E6	-50	500				
			I6	0	750	375
E7	-250	-40				
			I7	0	350	175
E8	-390	-180				

RI (time/intervals method)

Time max (years)	Time min (years)	Intervals	RI max (years)	Min (years)	RI preferred (years)
2166	1830	7	309	261	401

Note: Record may be incomplete, open-file report states “at least four, and possibly seven or more surface faulting earthquakes occurred during a 1630-2130 year interval.” Data and interval taken from Hayward Fault Working Group, OxCal model by Dawson and others (2008).

Hayward (South) **Latitude: 37.5563** **Longitude: -121.9739**

Tule Pond

Event	Calendar age (calibrated 2-sigma)	AD unless noted otherwise	Preferred	Interval ID	Min interval (years)	Max interval (years)	Mid ("preferred")
	Old	Young					
				OPEN	144	144	144
E1	1868	1868	1868				
				I1	83	211	143
E2	1657	1785	1725				
				I2	0	249	96
E3	1536	1737	1629				
				I3	0	352	154
E4	1385	1585	1475				
				I4	0	347	158
E5	1238	1408	1317				
				I5	0	403	183
E6	1005	1269	1134				
				I6	8	356	177
E7	913	997	957				
				I7	14	240	135
E8	757	899	822				
				I8	75	260	162
E9	639	682	660				
				I9	107	316	216
E9.5	366	532	444				
				I10	36	363	197
E10	169	330	247				
				I11	0	319	156
E11	11	172	91				

RI (time/intervals method)

Time max (years)	Time min (years)	Intervals	RI max (years)	RI min (years)	RI preferred (years)
1857	1696	11	169	154	162

Little Salmon (Onshore) **Latitude: 40.698423** **Longitude: -124.19822**

College of the Redwoods

Event	Calendar age (AD unless otherwise noted)	Preferred	Interval ID	Min interval (years)	Max interval (years)	Mid ("preferred")
	Old	Young				
			OPEN	212	500	356
MRE	1512	1800				

Little Salmon (Onshore) **Latitude: 40.655487** **Longitude: -124.18929**

Little Salmon Creek

Event	Calendar age (AD unless otherwise noted)	Preferred	Interval ID	Min interval (years)	Max interval (years)	Mid ("preferred")
	Old	Young				
			OPEN	212	500	356
MRE	1512	1800				

North Frontal (West) **Latitude: 34.360201** **Longitude: -116.871608**

Marble Canyon

Event	Calendar age (Calibrated 2-sigma)	Negative is BC	Preferred	Interval ID	Min interval (years)	Max interval (years)	Mid ("preferred")
	Old	Young					
				OPEN		11232	
MRE	-9220						

North Tahoe Latitude: 39.249051 Longitude: -119.963709

North Tahoe Basin

Event	Calendar age (calibrated 2-sigma)	AD unless noted otherwise	Preferred	Interval ID	Min interval (years)	Max interval (years)	Mid ("preferred")
	Old	Young					
				OPEN		512	
MRE	1500						

Panamint Valley Latitude: 35.858286 Longitude: -117.169492

Goler Wash

Event	Calendar age (calibrated 2-sigma)	AD unless noted otherwise	Preferred	Interval ID	Min interval (years)	Max interval (years)	Mid ("preferred")
	Old	Young					
				OPEN	512	612	562
MRE	1400	1500					

Puente Hills Latitude: 33.905282 Longitude: -118.110351

Santa Fe Springs—City of Bellflower

Event	Age (years bp, calibrated 2-sigma)		Preferred	Interval ID	Min interval (years)	Max interval (years)	Mid ("preferred")
	Old	Young					
				OPEN	200	300	250
Y	300	200					
				I1	2700	6100	4400
X	6300	3000					
				I2	300	5200	2750
W	8200	6600					

RI (time/intervals method)

Time max (years)	Time min (years)	Intervals	RI max (years)	RI min (years)	RI Preferred (years)
8000	6300	2	4000	3150	3575

Rodgers Creek-Healdsburg			Latitude: 38.2725		Longitude: -122.546 (Triangle G)	
			Triangle G/Beebe Ranch			
Event	Calendar age (calibrated 2-sigma)	AD unless noted otherwise	Interval ID	Min interval (years)	Max interval (years)	Mid ("preferred")
	Old	Young				
			OPEN	230	366	298
E1	1640	1776				

RI (time/intervals method)					
Time max (years)	Time min (years)	Intervals	RI max (yrs)	RI min (years)	RI preferred (years)
783	447	2	391.5	223.5	307.5

Note: to calculate the average interval used 3 earthquakes total during past 1100 years, based on correlation to other sites along strike.

Rodgers Creek-Healdsburg				Latitude: 38.272446		Longitude: -122.545763	
				Triangle G			
Event	Calendar age (calibrated 2-sigma)	AD unless noted otherwise	Preferred	Interval ID	Min interval (years)	Max interval (years)	Mid ("preferred")
	Old	Young					
				OPEN		322	297
MRE	1690		1715				

San Andreas (Big Bend) **Latitude: 34.8122** **Longitude: -118.9034**

Frazier Mountain

Event	Calendar age (calibrated 2-sigma)	AD unless noted otherwise	Preferred	Interval ID	Min interval (years)	Max interval (years)	Mid ("preferred")
	Old	Young					
				OPEN	155	155	155
1857	1857	1857	1857				
				I1	32	177	103
EQ2	1680	1825	1754				
				I2	60	272	171
EQ3	1553	1620	1583				
				I3	0	90	21
EQ4	1530	1599	1562				
				I4	0	90	24
EQ5	1509	1570	1538				
				I5	62	242	145
EQ6	1328	1447	1393				
				I6	118	339	229
EQ7	1108	1210	1164				
				I7	8	253	133
EQ8	957	1100	1031				

RI (time/intervals method)

Time max (years)	Time min (years)	Intervals	RI max (years)	RI min (years)	RI preferred (years)
900	757	7	129	108	119

San Andreas (Carrizo) **Latitude: 35.23428** **Longitude: -119.78871**

Bidart Fan

Event	Calendar age (calibrated 2-sigma)	AD unless noted otherwise	Preferred	Interval ID	Min interval (years)	Max interval (years)	Mid ("preferred")
	Old	Young					
				OPEN	155	155	155
A	1857	1857	1857				
				I1	34	226	144
B	1631	1823	1713				
				I2	0	243	99
C	1580	1640	1614				
				I3	0	130	49
D	1510	1612	1565				
				I4	35	162	103
E	1450	1475	1462				
				I5	0	115	45
F	1360	1452	1417				

RI (time/intervals method)

Time max (years)	Time min (years)	Intervals	RI max (years)	RI min (years)	RI preferred (years)
497	405	5	99.4	81	90

San Andreas (Coachella) **Latitude: 33.727354** **Longitude: -116.170074**

Coachella

Event	Calendar age (calibrated 2-sigma)	AD unless noted otherwise	Preferred	Interval ID	Min interval (years)	Max interval (years)	Mid ("preferred")
	Old	Young					
				OPEN	299	355	322
Coa-1	1657	1713	1690				
				I1	0	125	60
Coa-2	1588	1662	1630				
				I2	99	342	210
Coa-3 (poss.)	1320	1489	1420				
				I3	0	214	120
Coa-4	1275	1347	1300				
				I4	123	257	160
Coa-5	1090	1152	1140				
				I5	75	193	150
Coa-6 (poss.)	959	1015	990				
				I6	0	109	60
Coa-7	906	961	930				

RI (time/intervals method)

Time max (years)	Time min (years)	Intervals	RI max (years)	RI min (years)	RI preferred (years)
807	696	6	134.5	116	125.5

San Andreas (Coachella) **Latitude: 33.741128** **Longitude: -116.186175**

Indio

Event	Mean age (calendar years)	Standard error	Median	Interval ID	Min interval (years)	Max interval (years)	Mid ("preferred")
				OPEN			
Indio1	1680	23	1675				
				I1			
Indio2	1480	58	1475				
				I2			
Indio3	1300	45	1295				
				I3			
Indio4	1020	10	1015				

RI (time/intervals method)

Time max (years)	Time min (years)	Intervals	RI max (years)	RI min (years)	RI preferred (years)
693	627	3	231	209	220

San Andreas (Coachella)			Latitude: 33.836807			Longitude: -116.308798	
			Thousand Palms Oasis				
Event	Mean age (calendar years)	Standard error	Median	Interval ID	Min interval (years)	Max interval (years)	Mid ("preferred")
				OPEN			
TP1	1683	34	1674				
				I1			
TP2	1503	25	1494				
				I2			
TP3	1230	29	1223				
				I3			
TP4	982	79	978				
				I4			
TP5	824	29	830				

RI (time/intervals method)					
Time max (years)	Time min (years)	Intervals	RI max (years)	RI min (years)	RI preferred (years)
922	796	4	231	199	215

San Andreas (Mojave South) **Latitude: 34.45584** **Longitude: -117.887651**

Pallett Creek

Event	Calendar age (calibrated 2-sigma)	AD unless noted otherwise	Preferred	Interval ID	Min interval (years)	Max interval (years)	Mid ("preferred")
	Old	Young					
				OPEN	155	155	155
1857	1857	1857	1857				
				I1	13	141	44
1812	1716	1844	1813				
				I2	148	387	305
V	1457	1568	1508				
				I3	95	268	169
T	1300	1362	1339				
				I4	76	231	158
R	1131	1224	1181				
				I5	1	163	79
N	1061	1130	1102				
				I6	60	239	145
I	891	1001	957				
				I7	47	254	152
F	747	844	805				
				I8	0	146	77
D	698	754	728				

RI (time/intervals method)

Time max (years)	Time min (years)	Intervals	RI max (years)	RI min (years)	RI preferred (years)
1159	1103	8	145	138	141

San Andreas (Mojave South) **Latitude: 34.370541** **Longitude: -117.668229**

Wrightwood (young section)

Event	Mean age (calendar years)	Standard error	Median	Interval ID	Min interval (years)	Max interval (years)	Mid ("preferred")
				OPEN			
Historical	1857						
				I1			
Historical	1812						
				I2			
W3	1685	18	1681				
				I3			
W4	1536	13	1531				
				I4			
W5	1487	18	1478				
				I5			
W5T	1360	7	1361				
				I6			
W6	1264	29	1257				
				I7			
W7	1116	37	1111				
				I8			
W8	1016	27	1007				
				I9			
W9	850	20	852				
				I10			
W10	781	18	782				
				I11			
W11	722	11	722				
				I12			
W12	697	16	688				
				I13			
W13	634	31	628				
				I14			

San Andreas (Mojave South)—Continued.

W14	533	69	527		
			RI (time/intervals method)		
Time max (years)	**Time min (years)**	**Intervals**	**RI max (years)**	**RI min (years)**	**RI preferred (years)**
1393	1255	14	99.5	89.6	95

San Andreas (Mojave South) **Latitude: 34.370541** **Longitude: -117.668229**

Wrightwood (deep section)

Event	Age (calibrated 2-sigma)		Mean age (calendar years BCE)	Interval ID	Min interval (years)	Max interval (years)	Mid ("preferred")
	Old	Young					
W610	1635	1362	1503				
				I1	8	380	185
W600	1742	1627	1688				
				I2	40	237	86
W594	1864	1702	1774				
				I3	50	241	88
W592	1943	1814	1862				
				I4	68	163	54
W590	1977	1875	1916				
				I5	0	261	133
W570	2136	1988	2049				
				I6	48	196	79
W550.2	2184	2088	2128				
				I7	0	226	125
W520	2314	2198	2253				
				I8	67	175	56
W460	2373	2247	2309				
				I9	0	314	194
W410	2561	2450	2503				
				I10	0	220	107
W402	2670	2569	2610				
				I11	69	173	47
W390	2742	2601	2657				
				I12	47	206	89
W380	2807	2695	2746				
				I13	0	279	169
W350	2974	2883	2915				

San Andreas (Mojave South)—Continued.

RI (time/intervals method)					
Time max (years)	Time min (years)	Intervals	RI max (years)	RI min (years)	RI preferred (years)
1612	1248	13	124	96	110

San Andreas (North Coast) Latitude: 38.981221 Longitude: -123.676995

Alder Creek

Event	Calendar age (calibrated 2-sigma)	AD unless noted otherwise	Interval ID	Min interval (years)	Max interval (years)	Mid ("preferred")
	Old	Young				
			OPEN	106	106	106
MRE	1906	1906				
			I1	303	1226	764.5
2	680	1603				

RI (time/intervals method)					
Time max (years)	Time min (years)	Intervals	RI max (years)	RI min (years)	RI preferred (years)
1226	303	1	1226	303	764.5

Note: 4.9 meters offset in 1906, 3.1-4.6 meters in penultimate, used 4.3 meters as average displacement in table G5.

San Andreas (North Coast) **Latitude: 38.032** **Longitude: -122.7891**

Vedanta

Event*	Calendar age (calibrated 2-sigma)	AD unless noted otherwise	Interval ID	Min interval (years)	Max interval (years)	Mid ("preferred")
	Old	Young				
			OPEN	100	100	100
E1	1906	1906				
			I1	166	236	201
E2	1670	1740				
			I2	230	390	310
E3	1350	1440				
			I3	0	150	75
E4	1290	1380				
			I4	60	240	150
E5	1140	1230				
			I5	0	130	65
E6	1100	1165				
			I6	215	345	280
E7	820	885				
			I7	110	235	172.5
E8	650	710				
			I8	430	780	605
E9	-70	220				
			I9	50	570	310
E10 (BC)	-350	-120				
			I10	0	510	255
E11 (BC)	-630	-240				
			I11	30	750	390
E12 (BC)	-990	-660				

San Andreas (North Coast)—Continued.

			RI (time/intervals method)		
Time max (years)	Time min (years)	Intervals	RI max (years)	RI min (years)	RI preferred (years)
2896	2566	11	263	233	248

*Event ages taken from Zhang and others (2006)

Note: Earthquake intervals in Zhang and others (2006) differ from Zhang's (2006) Ph.D. thesis. Evidence for twelve earthquakes, including the 1906 earthquake, occurred since the deposition of a unit that is approximately 3,000 years old. Zhang interprets four pre-1906 events as rupturing the entire North Coast segment, including earthquakes in the following ranges: AD 1670–1740; AD 1290–1380; AD 1100–1165; and AD 650–710.

San Andreas (Offshore) **Latitude: 39.5167 Longitude: -124.333**

			Noyo Canyon turbidites			
Event	Calendar age (calibrated 2-sigma)	AD unless noted otherwise	Interval ID*	Min interval (years)	Max interval (years)	Mid ("preferred")*
			OPEN	100	100	100
E1	1906					
			I1			137
			I2			132
			I3			155
			I4			254
			I5			248
			I6			69
			I7			235
			I8			252
			I9			232
			I10			220
			I11			129
			I12			119
			I13			176
			I14			187

San Andreas (Offshore)—Continued.

			RI (time/intervals method)		
Time max (years)	Time min (years)	Intervals	RI max (years)	RI min (years)	RI preferred (years)
2890	2690	14	206	192	199

*Intervals from Goldfinger and others (2007)

San Andreas (Peninsula) Latitude: 37.47332 Longitude: -122.3116779

Filoli

Event	Calendar age (calibrated 2-sigma)	AD unless noted otherwise	Interval ID	Min interval (years)	Max interval (years)	Mid ("preferred")
	Old	Young				
			OPEN	106	106	106
MRE	1906	1906				
			I1	68	68	68
2*	1838	1838				

			RI (time/intervals method)		
Time max (years)	Time min (years)	Intervals	RI max (years)	RI min (years)	RI preferred (years)
68	68	1	68	68	68

* Hall and others, (1999) find evidence for 1906 and a penultimate earthquake. The June 1838 earthquake is their preferred interpretation for the penultimate event based on C^{14} constraints and historical descriptions of the event.

San Andreas (San Bernardino North) Latitude: 34.116751 Longitude: -117.141022

Plunge Creek

Event	Mean age (calendar years)	Standard error	Median	Interval ID	Min interval (years)	Max interval (years)	Mid ("preferred")
				OPEN			
Historical	1812						
				I1			
Plunge1	1619	48	1619				
				I2			
Plunge2	1499	114	1499				

San Andreas (San Bernardino North)—Continued.

RI (time/intervals method)					
Time max (years)	Time min (years)	Intervals	RI max (years)	RI min (years)	RI preferred (years)
427	199	2	213.5	99.5	156.5

San Andreas (San Bernardino North) **Latitude: 34.252306** **Longitude: -117.430282**

Pitman Canyon

Event	Mean age (calendar years)	Standard error	Median	Interval ID	Interval
				OPEN	200
Historical	1812				
				I1	119
Pit1.5*	1693				
				-	
Pit2	1704	50	1706		
				I2	
Pit3	1559	78	1567		
				I3	
Pit4	1437	70	1419		
				I4	
Pit5	1313	52	1305		
				I5	
Pit6	1173	81	1180		
				I6	
Pit7	931	91	942		

RI (time/intervals method)					
Time max (years)	Time min (years)	Intervals	RI max (years)	RI min (years)	RI preferred (years)
972	790	6	162	132	147

*Pit 1.5 is an alternative interpretation based on ^{14}C results.

San Andreas (San Bernardino South)				Latitude: 33.999664		Longitude: -116.860839	
			Burro Flats				
Event	Mean age (calendar years)	Standard error	Median	Interval ID	Min interval (years)	Max interval (years)	Mid ("preferred")
				OPEN			
Historical	1812						
				I1			
Burro2	1684	37	1673				
				I2			
Burro3	1500	23	1495				
				I3			
Burro4	1475	78	1478				
				I4			
Burro5	1347	21	1347				
				I5			
Burro6	1107	37	1098				
				I6			
Burro7	774	48	774				

RI (time/intervals method)					
Time max (years)	Time min (years)	Intervals	RI max (years)	RI min (years)	RI preferred (years)
1086	990	6	181	165	173

San Andreas (Santa Cruz Mountains) **Latitude: 36.909731** **Longitude: -121.62363**

Arano Flat/Mill Canyon

Event	Calendar age (calibrated 2-sigma)*	AD unless noted otherwise*	Interval ID	Min interval (years)	Max interval (years)	Mid ("preferred")
	Old	Young				
			OPEN	100	100	100
E1	1906	1906				
			I1	116	186	151
E2	1720	1790				
			I2	40	190	115
E3	1600	1680				
			I3	0	160	80
E4	1520	1620				
			I4	10	190	100
E5	1430	1510				
			I5	0	110	55
E6	1400	1470				
			I6	0	160	80
E7	1310	1400				
			I7	50	260	155
E8	1140	1260				
			I8	30	250	140
E9	1010	1110				

RI (time/intervals method)

Time max (years)	Time min (years)	Intervals	RI max (years)	RI min (years)	RI preferred (years)
896	796	8	112	100	106

*Values taken from OxCal generated model provided by T. Fumal (written commun., 2007)

San Andreas (Santa Cruz Mountains) **Latitude: 37.000318** **Longitude: -121.741757**

Hazel Dell

Event	Calendar age (calibrated 2-sigma)	AD unless noted otherwise	Preferred	Interval ID	Min interval (years)	Max interval (years)	Mid ("preferred")
	Old	Young					
				OPEN	106	106	106
Event 1	1906	1906	1906				
				I1	16	41	16
Event 2	-	-	1890 (preferred) or 1865 (alternative)				
				I2	0	52	52
Event 3	-	-	1838 (preferred) or 1865 (alternative)				
				I3*	520	1105	288
Event 4*	760	1318	1093				

RI (time/intervals method)

Time max (years)	Time min (years)	Intervals	RI max (years)	RI min (years)	RI preferred (years)
1146	588	3	382	196	289

*Authors interpret a depositional hiatus between E3 and E4; record may not be complete and interval may not be accurate.

Note: values from Streig and others, in press, Bulletin of the Seismological Society of America.

San Andreas (Santa Cruz Mountains) **Latitude: 36.946063** **Longitude: -121.679612**

Mill Canyon

Event	Calendar age (calibrated 2-sigma)	AD unless noted otherwise	Preferred	Interval ID	Min interval (years)	Max interval (years)	Mid ("preferred")
	Old	Young	Preferred				
				OPEN	106	106	106
E1	1906	1906	1906				
				I1	68	158	68
E2			1838 (preferred) or 1748 (alternative)				
				I2	29	179	152
E3	1659	1719	1686				
				I3	54	265	164
E4	1454	1605	1522				

RI (time/intervals method)

Time max (years)	Time min (years)	Intervals	RI max (years)	RI min (years)	RI preferred (years)
452	301	3	150	100	377

San Cayetano				Latitude: 34.40922		Longitude: -118.81442	
				Piru			
Event	Calendar age (calibrated 2-sigma)	AD unless noted otherwise	Preferred	Interval ID	Min interval (years)	Max interval (years)	Mid ("preferred")
	Old	Young					
				OPEN		352	
MRE	1660						

San Gorgonio Pass				Latitude: 33.932764		Longitude: -116.764564	
				Cabazon			
Event	Age (years before present)		Preferred	Interval ID	Min interval (years)	Max interval (years)	Mid ("preferred")
	Old	Young					
				OPEN	600	800	700
MRE	800	600					

San Gregorio (North)			Latitude: 37.520948		Longitude: -122.513702	
			Seal Cove			
Event	Calendar age (calibrated 2-sigma)	AD unless noted otherwise	Interval ID	Min interval (years)	Max interval (years)	Mid ("preferred")
	Old	Young				
			OPEN	231	736	483.5
MRE	1270	1775				
			I1	130	1175	652.5
2	600	1400				

RI (time/intervals method)					
Time max (years)	Time min (years)	Intervals	RI max (years)	RI min (years)	RI referred (years)
1175	670	1	1175	670	923

San Jacinto (Anza)				**Latitude: 33.68501558**		**Longitude: -116.8234926**	
				Blackburn Canyon			
Event	**Calendar age (calibrated 2-sigma)**	**AD unless noted otherwise**	**Preferred**	**Interval ID**	**Min interval (years)**	**Max interval (years)**	**Mid ("preferred")**
	Old	Young					
				OPEN			213
MRE*			1800*				

*MRE from Buga and others (2011).

San Jacinto (Anza)			**Latitude: 33.6153**		**Longitude: -116.7091**	
			Hog Lake			
Event	**Calendar age range (calibrated 2-sigma)**	**AD, unless noted otherwise**	**Interval**	**Min interval (years)***	**Max interval (years)***	**Mid ("preferred")**
	Old	Young				
			OPEN	95	95	95
E1	-	1918**				
			I1	288	398	343
E2	1520	1630				
			I2	170	340	255
E3	1290	1350				
			I3	0	70	35
E4	1280	1350				
			I4	0	80	40
E5	1270	1300				
			I5	0	160	80
E6	1140	1290				
			I6	0	310	155
E7	980	1160				
			I7	0	810	405
E8	350	1000				
			I8	0	800	400

San Jacinto (Anza)—Continued.

Event	Calendar age range (calibrated 2-sigma)	AD, unless noted otherwise	Interval	Min interval (years)*	Max interval (years)*	Mid ("preferred")
E9	200	850				
			I9	0	750	375
E10	100	260				
			I10	190	610	400
E11 (B.C.E.)	350	90				
			I11	0	420	210
E12 (B.C.E.)	510	230				
			I12	100	650	375
E13 (B.C.E.)	880	610				
			I13	480	960	720
E14 (B.C.E.)	1570	1360				
E15	Unconstrained					
E16	Unconstrained					

RI (time/intervals method)					
Time max (years)	Time min (years)	Intervals	RI max (years)	RI min (years)	RI preferred (years)
4000	3500	15	267	233	250

* RI data from Rockwell and others (2006) abstract (16 earthquakes in 3.5–4.0 ka).

** E1 is 1918, from unpublished new work (T. Rockwell, written commun., 2013).

San Jacinto (Claremont) **Latitude: 33.900322** **Longitude: -117.089184**

Mystic Lake

Event	Calendar age (calibrated 2-sigma)	AD unless noted otherwise	Preferred	Interval ID	Min interval (years)	Max interval (years)	Mid ("preferred")
	Old	Young					
				OPEN	160	269	219
MRE	1744	1853	1799				
				I1	0	188	
E2	1665	1820	1743				
				I2	49	299	
E3	1521	1616	1569				
				I3	76	213	
E4	1403	1445	1424				
				I4	0	172	
E5	1273	1419	1346				
				I5	312	612	
E6	807	961	884				
				I6	0	382	
E7	579	846	712				

RI (time/intervals method)

Time max (years)	Time min (years)	Intervals	RI max (years)	RI min (years)	RI preferred (years)
1274	898	6	212	150	181

Note: Values from table 3 in Onerdonk and others (2013); this fault was added during review (reference became available after compilation was complete), and was too late to integrate into the model.

San Jacinto (Clark) **Latitude: 33.309305** **Longitude: -116.192930**

Lute Ridge

Event	Calendar age (calibrated 2-sigma)	AD unless noted otherwise	Preferred	Interval ID	Min interval (years)	Max interval (years)	Mid ("preferred")
	Old	Young					
				OPEN			222
MRE			1790				

San Jacinto (Superstition Mountain) **Latitude: 32.9975** **Longitude: -115.9436**

Superstition Mountain

Event	Calendar age range (calibrated 2-sigma)	AD unless noted otherwise	Interval	Min interval (years)	Max interval (years)	Mid ("preferred")
	Old	Young				
			OPEN	366	566	466
E1	1440	1640				
			I1	0	360	180
E2	1280	1640				
			I2	0	820	410
E3	820	1280				
			I3	0	record likely incomplete prior to E3	
E4*	4670 BC	964				

RI (time/intervals method)

Time max (years)	Time min (years)	Intervals	RI max (years)	RI min (years)	RI preferred (years)
823	476	2	412	238	325

* Constraining lower date: A.D. 817–964, RI calculated from this and E1 event age.

Note: Event ages and recurrence from Gurrola and Rockwell, 1996.

Sierra Madre **Latitude: 34.128521** **Longitude: -117.810299**

San Dimas

Event	Calendar age (calibrated 2-sigma)	AD unless noted otherwise	Preferred	Interval ID	Min interval (years)	Max interval (years)	Mid ("preferred")
	Old	Young					
				OPEN		15541	
MRE	13,529 BC - 11,903 BC						

Whittier **Latitude: 33.9303** **Longitude: -117.8437**

Event	Age (years BP, calibrated 2-sigma)	AD unless noted otherwise	Interval	Min interval (years)	Max interval (years)	Mid ("preferred")
	Young	Old				
			OPEN	1400	2200	1800
E1	1400	2200				
			I1	800	2000	1400
E2	3000	3400				

RI (time/intervals method)

Time max (years)	Time min (years)	Intervals	RI max (years)	RI min (years)	RI preferred (years)
2000	800	1	2000	800	1400

Table G3. Paleoseismic ages and intervals from Uniform California Earthquake Forecast, version 2 that have been superseded by newer data.

Elsinore (Temecula)			**Latitude: 33.41**		**Longitude: -117.04**	
			Temecula OLD			
Event	**Age of MRE in calendar years (calibrated 2-sigma)**	**AD unless noted otherwise**	**Interval**	**Min interval (years)**	**Max interval (years)**	**Mid ("preferred")**
X	1650	1810	OPEN	196	356	276
Incomplete record until Event T						
	In years B.P. below					
	Young	Old				
Event T	2700	3300				
			I1	0	800	400
Event P	3000	3500				
			I2	0	1500	750
Event L	3500	4500				
			I3	500	Unconstrained	Unconstrained
Event H	4500	>4500				

RI (time/intervals method)

Time max (years)	**Time min (years)**	**Intervals**	**RI max (years)**	**RI min (years)**	**RI preferred (years)**
1800	1200	3	600	400	500

Event H reported as shortly before 4500. Can use this as a minimum recurrence interval between L and H.

Event ages as reported by Vaughan and others (1999).

Hayward (South)			**Latitude: 37.5563 (Tule Pond) OLD**		**Longitude: -121.9739**	
Event	**Calendar age (calibrated 2-sigma)***	**AD unless noted otherwise***	**Interval ID**	**Min interval (years)**	**Max interval (years)**	**Mid ("preferred")**
	Old	Young				
			OPEN	138	138	138
E1	1868	1868				
			I1	78	218	148
E2	1650	1790				
			I2	0	260	130
E3	1530	1740				
			I3	0	360	180
E4	1380	1590				
			I4	0	360	180
E5	1230	1410				
			I5	0	410	205
E6	1000	1270				
			I6	0	360	180
E7	910	1010				
			I7	10	260	135
E8	750	900				
			I8	70	510	290
E9	390	680				
			I9	0	400	200
E10	280	640				
			I10	0	450	225
E11	190	550				

RI (time/intervals method)					
Time max (years)	**Time min (years)**	**Intervals**	**RI max (years)**	**RI min (years)**	**RI preferred (years)**
1678	1318	10	168	132	150

*Values taken from OxCal-generated model provided by Lienkaemper prior to publication of the data presented in G2 that supersedes this data.

San Andreas (Carrizo)

			Carrizo combined				
Event	Mean age (calendar years)	Standard error	Median	Interval ID	Min interval (years)	Max interval (years)	Mid ("preferred")
				OPEN			
Historical	1857						
				I1			
Carr2shv	1571	116	1596				
				I2			
Carr3shv	1384	77	1373				
				I3			
Carr4shv	1277	103	1318				
				I4			
Carr5shv	1078	82	1050				
				I5			

San Andreas (Mojave South)

Pallett Creek OLD

Event	Mean age (calendar years)	Standard error	Median	Interval ID	Min interval (years)	Max interval (years)	Mid ("preferred")
				OPEN			
Historical	1857						
				I1			
Historical	1812						
				I2			
V	1547	31	1546				
				I3			
T	1360	7	1361				
				I4			
R	1084	16	1087				
				I5			
N	1067	16	1065				
				I6			
I	956	19	952				
				I7			
F	842	17	846				
				I8			
D	764	7	758				
				I9			
C	645	12	646				

San Andreas (Mojave South)				Latitude: 34.252306		Longitude: 117.430282	
				Pitman Canyon OLD			
Event	Mean age (calendar years)	Standard error	Median	Interval ID	Min interval (years)	Max interval (years)	Mid (aka "preferred")
				OPEN			
Historical	1812						
				I1			
Pit2	1704	50	1706				
				I2			
Pit3	1559	78	1567				
				I3			
Pit4	1437	70	1419				
				I4			
Pit5	1313	52	1305				
				I5			
Pit6	1173	81	1180				
				I6			
Pit7	931	91	942				

San Andreas (Mojave South)				Latitude: 34.370541 Wrightwood OLD		Longitude: 117.668229	
Event	Mean age (calendar years)	Standard error	Median	Interval ID	Min interval (years)	Max interval (years)	Mid ("preferred")
				OPEN			
Historical	1857						
				I1			
Historical	1812						
				I2			
W3	1685	18	1681				
				I3			
W4	1536	13	1531				
				I4			
W5	1487	18	1478				
				I5			
W5T	1360	7	1361				
				I6			
W6	1264	29	1257				
				I7			
W7	1116	37	1111				
				I8			
W8	1016	27	1007				
				I9			
W9	850	20	852				
				I10			
W10	781	18	782				
				I11			
W11	722	11	722				
W12	697	16	688				
				I12			
W13	634	31	628				
				I13			
W14	533	69	527				

San Andreas (Santa Cruz Mountains)			**Latitude: 36.9415**		**Longitude: 121.6729**	
			(Arano Flat/Mill Canyon) OLD			
Event	**Calendar age (calibrated 2-sigma)**	**AD unless noted otherwise**	**Interval ID**	**Min interval (years)**	**Max interval (years)**	**Mid ("preferred")**
	Old	Young				
			OPEN	100	100	100
E1	1906	1906				
			I1	116	186	151
E2	1720	1790				
			I2	40	190	115
E3	1600	1680				
			I3	0	160	80
E4	1520	1620				
			I4	10	190	100
E5	1430	1510				
			I5	0	110	55
E6	1400	1470				
			I6	0	160	80
E7	1310	1400				
			I7	50	260	155
E8	1140	1260				
			I8	30	250	140
E9	1010	1110				

RI (time/intervals method)					
Time max (years)	**Time min (years)**	**Intervals**	**RI max (years)**	**RI min (years)**	**RI preferred (years)**
896	796	8	112	100	106

*Values taken from OxCal generated model provided by T. Fumal prior to publication of the data presented in G2 that supersedes this data.

San Gregorio (North)			**Latitude: 37.5207 (Seal Cove) OLD**		**Longitude: 122.5135**	
Event	**Calendar age (calibrated 2-sigma)**	**AD unless noted otherwise**	**Interval ID**	**Min interval (years)**	**Max interval (years)**	**Mid ("preferred")**
	Old	Young				
			OPEN	230	736	483
E1	1270	1776				
			I1	0	1156	578
E2	620	1400				

Table G4. Overlap of the age of paleoearthquakes along multisite faults.

[Values in cells above and right of dash marks are the number of age overlaps for two sites. Values in cells below dash marks are the number of events in the time interval common to the two sites. The first number is from the site to the left, the second number is from the site above. So, for example: Whittier has a 2-event record and 2 are in a common time period with Temecula, which has 5 total events but only 3 in the common interval]

Elsinore

	Latitude	Longitude	Total number of events	Whittier	Glen Ivy	Temecula	Julian—Lake Henshaw S	Julian
Whittier	33.93030	-117.84370	2	-	0	1	1	2
Glen Ivy	33.77010	-117.49090	6	6, 1	-	1	1	0
Temecula	33.41000	-117.04000	5	3, 2	2, 6	-	0	1
Julian - Lake Henshaw S	33.218126	-116.73993	1	1, 1	1, 6	1, 1	-	1
Julian	33.20710	-116.72730	2	2, 2	1, 6	2, 3	1, 1	-

San Jacinto

	Latitude	Longitude	Total number of events	Clark (Blackburn Canyon)	Hog Lake	Clark Rev (Lute Ridge)	Superstition Mountains
Clark (Blackburn Canyon)	33.615300	-116.709100	1	-	1	1	0
Hog Lake	33.685016	-116.823493	16	16, 1	-	1	4
Clark Rev (Lute Ridge)	33.309305	-116.192930	1	1, 1	1, 1	-	0
Superstition Mt	32.997500	-115.943600	4	1, 1	4, 16	0, 0	-

Southern San Andreas

	Latitude	Longitude	Total number of events	Carrizo Bidart Fan	Frazier	Pallett Creek	Wrightwood	Pitman Canyon	Plunge Creek	Burro Flats	Thousand Palms Oasis	Indio	Coachella
Carrizo Bidart Fan	35.23428	-119.78871	6	-	5	4	5	4	2	3	2	2	3
Frazier	34.8122	-118.9034	8	8, 6	-	6	6	5	3	4	4	4	5
Pallett Creek	34.45584	-117.887651	9	4, 6	7, 8	-	8	5	2	5	5	2	3
Wrightwood	34.370541	-117.668229	15 (29 incl.deep section)	6, 6	9, 8	12, 9	-	7	3	7	5	4	5
Pitman Canyon	34.252306	-117.430282	6	6, 6	8, 8	8, 8	8, 10	-	3	6	4	4	6
Plunge Creek	34.116751	-117.141022	3	3, 6	3, 6	3, 3	3, 5	3, 5	-	3	2	2	2
Burro Flats	33.999664	-116.860839	7	5, 6	6, 8	7, 8	7, 12	7, 8	4, 3	-	3	3	4
Thousand Palms Oasis	33.836807	-116.308798	5	2, 6	4, 8	5, 8	5, 11	5, 8	2, 3	5, 7	-	4	3
Indio	33.741128	-116.186175	4	2, 6	4, 8	4, 5	4, 9	4, 8	2, 3	4, 6	4, 4	-	4
Coachella	33.727354	-116.170074	7	3, 6	7, 8	7, 7	7, 9	7, 8	3, 3	7, 6	7, 4	4, 6	-

Table G4—Continued.

Northern San Andreas

	Latitude	Longitude	Total number of events	North Coast Alder Creek	North Coast Vendanta	Peninsular Filoli	Hazel Dell	Mill Canyon	Arano Flat
North Coast Alder Creek	38.981331	-123.676995	2	-	2	1	2	2	2
North Coast Vendanta	38.032	-122.7891	12	8, 2	-	1	1	2	6
Peninsula Filoli	37.47332	-122.3116779	2	2, 1	2, 1	-	2	2	1
Hazel Dell	37.000318	-121.741757	4	4, 2	4, 2	3, 2	-	3	2
Mill Canyon	36.946053	-121.679612	4	4, 2	3, 2	2, 2	4, 4	-	4
Arano Flat	36.909731	-121.62363	9	9, 2	9, 6	1, 2	5, 4	5, 4	-

Hayward

	Latitude	Longitude	Total number of events	Mira Vista	Tyson Lagoon
Mira Vista	37.9306	-122.2977	7	-	6
Tyson Lagoon	37.5563	-121.9739	12	12, 6	-

Garlock

	Latitude	Longitude	Total number of events	Twin Lakes	El Paso Peaks	Searles Valley
Twin Lakes	34.9868	-118.508	5	-	4	1
El Paso Peaks	35.4441	-117.6815	6	5, 5	-	1
Searles Valley	35.523424	-117.372841	1	1, 2	1, 1	-

Little Salmon

	Latitude	Longitude	Total number of events	College of the Redwoods	Little Salmon Creek
College of the Redwoods	40.698423	-124.19822	1	-	1
Little Salmon Creek	40.655487	-124.18929	1	1, 1	-

Table G4—Continued.

Green Valley

	Latitude	Longitude	Total number of events	Mason Road	Lopes Ranch
Mason Road	38.240934	-122.163795	4	-	1
Lopes Ranch	38.132456	-122.122902	3	1, 4	-

Table G5. Probability of rupture overlap along multi-site faults based on average paleoearthquake offset.

[Values below the gray boxes are distances between sites (in kilometers), values above gray boxes are probability of offset between two sites. So: Whittier is 37.19 km from Glen Ivy, and there is a 0.28 probability of rupture being shared between Glen Ivy and Whittier. Bold values are measured; non-bold values are calculated; mm/yr, millimeters per year; yrs, years; m, meters]

Elsinore

Site	Slip rate (mm/yr)	Average interval (years)	Average offset (m)	Latitude	Longitude	Whittier	Glen Ivy	Temecula	Julian-5	Julian—Lake Henshaw S	Julian
Whittier	**3**	**1600**	4.80	33.930300	-117.843700	1.00	0.28	0.32	0.06	0.38	0.43
Glen Ivy	**5**	**174**	0.87	33.770100	-117.490900	37.19	1.00	0.35	0.09	0.09	0.08
Temecula	**5**	**500**	2.50	33.410000	-117.040000	95.04	57.85	1.00	0.59	0.73	0.68
Julian-5	**3**	283	**0.85**	33.243444	-116.786003	125.01	87.82	29.97	1.00	0.95	0.95
Julian - Lake Henshaw S	**3**	**1200**	3.60	33.218126	-116.739925	130.14	92.95	35.10	5.13	1.00	0.99
Julian	**3**	**1625**	4.88	33.207100	-116.727300	131.83	94.64	36.79	6.82	1.69	1.00

San Jacinto

Site	Slip rate (mm/yr)	Average interval (years)	Average offset (m)	Latitude	Longitude	Hog Lake	Anza-1	Clark Black-burn Canyon	Anza-5	Clark-0	Clark-1	Clark-4	Clark (Lute Ridge)	Super-stition Mt
Hog Lake	**14**	**250**	3.50	33.685016	-116.823493	1.00	0.99	0.84	0.75	0.70	0.66	0.42	0.32	0.57
Anza-1	**14**	136	1.90	33.676686	-116.812736	1.36	1.00	0.91	0.65	0.59	0.57	0.17	0.23	0.28
Clark (Black-burn Canyon)	**14**	**94**	1.32	33.615300	-116.709100	13.14	11.78	1.00	0.71	0.68	0.58	0.23	0.20	0.15
Anza-5	**14**	154	**2.15**	33.510107	-116.547197	32.16	30.80	19.02	1.00	0.89	0.82	0.50	0.43	0.30
Clark-0	**8**	281	**2.25**	33.4691300	-116.479585	39.91	38.55	26.77	7.75	1.00	0.89	0.62	0.56	0.36
Clark-1	**8**	313	**2.50**	33.4278580	-116.411539	47.72	46.36	34.58	15.56	7.81	1.00	0.71	0.65	0.42
Clark-4	**4**	325	**1.30**	33.3127287	-116.205162	70.77	69.41	57.63	38.61	30.86	23.05	1.00	0.99	0.40

Table G5: San Jacinto—continued.

Site	Slip rate (mm/yr)	Average interval (years)	Average offset (m)	Latitude	Longitude	Hog Lake	Anza-1	Clark Black-burn Canyon	Anza-5	Clark-0	Clark-1	Clark-4	Clark (Lute Ridge)	Super-stition Mt
Clark (Lute Ridge)	**4**	**222**	0.89	33.309305	-116.192930	71.97	70.61	58.83	39.81	32.06	24.25	1.2	1.00	0.40
Superstition Mt	**6**	**325**	1.95	32.997500	-115.943600	113.58	112.22	100.44	81.42	73.67	65.86	42.81	41.61	1.00

Southern San Andreas

Site name	Abbreviation	Slip rate (mm/yr)	Average interval (years)	Average offset (m)	Latitude	Longitude
Cholame-8	CH	**34**	65	**2.20**	35.65162	-120.20197
Carrizo Bidart	CB	**34**	**99**	3.37	35.23428	-119.78871
Carrizo-1	C1	**34**	119	**4.05**	35.23846	-119.78729
Carrizo-5	C5	**34**	121	**4.10**	35.04907	-119.56036
Carrizo-6	C6	**34**	135	**4.60**	35.00640	-119.49824
Frazier	FZ	**34**	**109**	3.71	34.81220	-118.90340
Mojave S-2	M2	**32.5**	89	**2.90**	34.63846	-118.34692
Mojave S-3	M3	**32.5**	89	**2.90**	34.61433	-118.28205
Pallett Creek	PA	**32.5**	**128**	4.17	34.45584	-117.88765
Wrightwood	WW	**32.5**	**101**	**3.28**	34.37054	-117.66823
Pitman Canyon	PI	**19**	**147**	2.39	34.25231	-117.43028
Plunge Creek	PL	**13**	**157**	2.03	34.11675	-117.14102
Burro Flats	BF	**13**	**173**	2.25	33.99966	-116.86084
Thousand Palms	TP	**10**	**215**	2.15	33.83681	-116.30880
Indio	IN	**10**	**220**	2.20	33.74113	-116.18618
Coachella	CO	**20**	**155**	3.09	33.72735	-116.17007
Coachella-4	C4	**20**	150	**3.00**	33.63701	-116.06091
Salt Creek	SC	**23**	**~150**	3.45	33.44564	-115.84040
Coachella-10	C10	**20**	160	**3.20**	33.43470	-115.81447

Table G5: Southern San Andreas—continued.

Site	CH	CB	C1	C5	C6	FZ	M2	M3	PA	WW	PI	PL	BF	TP	IN	CO	C4	SC	C10
CH	1.00	0.56	0.61	0.44	0.45	0.19	0.08	0.07	<.05	<.05	<.05	<.05	<.05	<.05	<.05	<.05	<.05	<.05	<.05
CB	59.6	1.00	0.99	0.81	0.79	0.46	0.22	0.21	0.17	0.12	0.07	<.05	<.05	<.05	<.05	<.05	<.05	<.05	<.05
C1	60.1	0.48	1.00	0.85	0.81	0.47	0.25	0.24	0.18	0.11	0.08	<.05	<.05	<.05	<.05	<.05	<.05	<.05	<.05
C5	89.6	30.0	29.5	1.00	0.98	0.66	0.35	0.34	0.28	0.16	0.11	0.06	<.05	<.05	<.05	<.05	<.05	<.05	<.05
C6	97.0	37.3	36.9	7.4	1.00	0.70	0.41	0.38	0.29	0.19	0.14	0.08	<.05	<.05	<.05	<.05	<.05	<.05	<.05
FZ	155.3	95.7	95.2	65.8	58.4	1.00	0.68	0.63	0.48	0.34	0.23	0.13	0.09	<.05	<.05	<.05	<.05	<.05	<.05
M2	209.7	150.1	149.6	120.2	112.8	54.4	1.00	0.99	0.74	0.56	0.31	0.23	0.13	0.07	0.06	0.07	<.05	<.05	<.05
M3	216.3	156.6	156.2	126.7	119.3	60.9	6.5	1.00	0.75	0.61	0.34	0.24	0.15	0.09	0.07	0.08	0.06	<.05	<.05
PA	256.5	196.8	196.4	166.9	159.5	101.1	46.7	40.2	1.00	0.87	0.70	0.53	0.37	0.20	0.18	0.18	0.15	0.12	0.12
W																			
W	278.7	219.1	218.6	189.1	181.7	123.4	69.0	62.5	22.3	1.00	0.81	0.58	0.40	0.10	0.17	0.21	0.17	0.13	0.14
PI	304.2	244.6	244.1	214.6	207.3	148.9	94.5	88.0	47.8	25.5	1.00	0.52	0.45	0.21	0.18	0.22	0.19	0.15	0.14
PL	334.8	275.2	274.7	245.3	237.9	179.5	125.1	118.6	78.4	56.1	30.6	1.00	0.69	0.30	0.23	0.30	0.26	0.20	0.17
BF	363.8	304.2	303.7	274.2	266.9	208.5	154.1	147.6	107.4	85.1	59.6	29.0	1.00	0.48	0.40	0.46	0.36	0.30	0.27
TP	418.0	358.3	357.9	328.4	321.0	262.6	208.2	201.7	161.5	139.3	113.7	83.1	54.1	1.00	0.83	0.85	0.78	0.58	0.50
IN	433.5	373.9	373.4	343.9	336.5	278.2	223.8	217.3	177.1	154.8	129.3	98.7	69.7	15.6	1.00	0.99	0.83	0.68	0.64
CO	435.6	376.0	375.5	346.1	338.7	280.3	225.9	219.4	179.2	156.9	131.4	100.8	71.8	17.7	2.1	1.00	0.86	0.74	0.74
C4	449.9	390.3	389.8	360.3	352.9	294.5	240.1	233.6	193.4	171.2	145.7	115.1	86.1	31.9	16.4	14.3	1.00	0.85	0.76
SC	475.8	416.2	415.7	386.2	378.8	320.5	266.1	259.5	219.3	197.1	171.6	141.0	112.0	57.8	42.3	40.2	25.9	1.00	0.99
C10	478.5	418.9	418.4	388.9	381.5	323.2	268.8	262.2	222.0	199.8	174.3	143.7	114.7	60.5	45.0	42.9	28.6	2.7	1.00

Northern San Andreas

Site	Slip rate (mm/yr)	Average interval (years)	Average offset (m)	Latitude	Longitude	North Coast Alder Creek	North Coast Vendanta	Peninsula Filoli	Hazel Dell	Mill Canyon	Arano Flat
North Coast Alder Creek	**24**	179	**4.3**	38.981331	-123.676995	1.00	0.60	0.26	<.05	<.05	<.05
North Coast Vendanta	**24**	**248**	5.95	38.032000	-122.789100	130.68	1.00	0.58	0.28	0.27	0.24
Peninsular Filoli	**17**	**87**	1.48	37.473320	-122.311678	205.43	74.75	1.00	0.28	0.23	0.19
Hazel Dell	**17**	**115**	1.96	37.000318	-121.741757	278.21	147.53	72.78	1.00	0.92	0.78
Mill Canyon	**17**	**123**	2.08	36.946053	-121.679612	286.37	155.69	80.94	8.16	1.00	0.96
Arano Flat	**17**	**106**	1.80	36.909731	-121.623630	292.78	162.10	87.35	14.57	6.41	1.00

Table G5—Continued.

Hayward

Site	Slip rate (mm/yr)	Average interval (years)	average offset (m)	Latitude	Longitude	Mira Vista	Tyson Lagoon
Mira Vista	**9**	**401**	3.61	37.930600	-122.297700	1.00	0.57
Tyson Lagoon	**9**	**160**	1.44	37.556300	-121.973900	50.35	1.00

Garlock

Site	Slip rate (mm/yr)	Average interval (years)	Average offset (m)	Latitude	Longitude	Twin Lakes	West-10	West-12	El Paso Peaks	Searles Valley	Central-15
Twin Lakes	**6**	**1159**	6.95	34.986800	-118.508000	1.00	0.86	0.78	0.65	0.39	0.24
West-10	**7.6**	454	**3.45**	35.13590678	-118.219538	31.05	1.00	0.86	0.68	0.43	0.35
West-12	**7.6**	461	**3.50**	35.20431919	-118.091091	44.98	13.93	1.00	0.73	0.55	0.43
El Paso Peaks	**7**	**1276**	8.93	35.444100	-117.681500	90.72	59.67	45.74	1.00	0.83	0.63
Searles Valley	**7**	**522**	3.65	35.523424	-117.372841	120.03	88.98	75.05	29.31	1.00	0.86
Central-15	**7**	443	**3.10**	35.56946148	-117.149948	140.84	109.79	95.86	50.12	20.81	1.00

Little Salmon

Site	Slip rate (mm/yr)	Average interval (years)	Average offset (m)	Latitude	Longitude	College of the Redwoods	Little Salmon Creek
College of the Redwoods	**4.5**	**356**	1.60	40.698423	-124.198220	1.00	0.96
Little Salmon Creek	**4.5**	**356**	1.60	40.655487	-124.189290	4.83	1.00

Green Valley

Site	Slip rate (mm/yr)	Average interval (years)	Average offset (m)	Latitude	Longitude	Mason Road	Lopes Ranch
Mason Road	**4**	**201**	0.80	38.240934	-115.840508	1.00	0.74
Lopes Ranch	**4**	506	**2.03**	38.132456	-122.122902	12.58	1.00